VERIFICATION OF LONG RANGE QUANTUM PHASE COHERENCE IN SUPERCONDUCTING TIN UTILIZING ELECTROMAGNETICALLY STABILIZED JOSEPHSON JUNCTIONS

Thesis by
Lorin Lee Vant-Hull

In Partial Fulfillment of the Requirements

For the Degree of
Doctor of Philosophy

California Institute of Technology
Pasadena, California
1967
(Submitted December 2 , 1966)

ACKNOWLEDGMENTS

It is a pleasure to acknowledge the continuing support and encouragement of my primary research advisor, Dr. James E. Mercereau, whose original suggestion led to this work. The many hours spent together in laboratory work and in discussion have been most rewarding. Recognition is due to the several people who, under one circumstance or another also served in the position of research advisor: Drs. Pellam, DuMond, Hildebrandt, and Anderson. It is a pleasure to recall numerous revealing luncheon engagements with Dr. Feynman.

Financial assistance has been generously provided by the Alfred P. Sloan Foundation, the General Electric Company and the Ford Motor Company.

The patience and understanding of my wife and children havenot only made my career as a graduate student possible, but rewarding as well.

ABSTRACT

de Broglie wave interferometers have been constructed, successfully utilizing extended superconducting links of tin to couple coherently the quantum phases of two Josephson junctions. The current transmitted by these devices was periodic in the enclosed flux (periodicity $(.9 \pm .3)\frac{h}{2e}$) demonstrating unambiguously coherence of the superconducting order parameter over 1.33 meters.

We may define a "normal" Josephson junction as one for which the quantum mechanical coupling energy is insufficient to overcome the disruptive effects of noise. Consequently, the relative phase of the coupled superconductors is not stabilized and the "zero voltage" Josephson current fluctuates, (bandwidth $\sim 2eV_{noise}/h$) averaging to zero. Two such "normal" junctions have been coupled to an electromagnetic cavity formed by the superconducting arms of a quantum interferometer (junction separation 1.33 meters). With an applied steady voltage such that the Josephson current excites a normal mode of the cavity, a coherent radiation field is built up. This coherent radiation feeds back to the junctions forcing time coherence on the phase precession, resulting in a dynamic stabilization of the junctions.

Under these conditions a series of "constant voltage steps" has been observed in the I-V characteristic of one interferometer. The Josephson frequency associated with these steps is shown to be characteristic of the electromagnetic resonant modes of the cavity. Frequency modulation analysis, combined with a detailed analysis of the cavity-junction combination, predicts such maxima in the tunneling of pairs when a "selection rule", (m + n) even, is obeyed. Here m/2 is the number of flux quanta (h/2e) linking the interferometer and n is the order of the cavity resonance excited. Experimental confirmation of the detailed predictions of the analysis is presented.

TABLE OF CONTENTS

I. INTRODUCTION

In the years since Planck successfully explained black body radiation by quantizing the energy levels of the individual oscillators, the concepts of quantum mechanics have been applied with universal success to the entire field of atomic behavior. Attempts to extend the theory to include nuclear process have been less successful, partly because of the strength of the nuclear interaction.

In contrast, the correspondence principle guarantees that quantum mechanics may be applied to a macroscopic system occupying a large number of quantum states. The probabilities predicted for such a system generally have such a narrow range of uncertainty and are so closely spaced that they justify the use of the classical analysis. The small size of the quantum of action, $\hbar$, in the uncertainty relations and wave equations of quantum mechanics leads to a negligible effect in the macroscopic system and the corresponding classical and quantum mechanical treatments produce converging results. The possibility of a system existing with a macroscopic number of particles in a single coherent quantum state, however, leads to a new situation. Quantization of the wave functions of such a system leads to final states which are still sharply defined. However, their spacing may now be macroscopic, an effect completely outside the domain of classical physics. This macroscopic spacing of states is a purely quantum effect, in fact the spacing involves the size of $\hbar$ directly. Thus, we have a macroscopic system to which it is not valid to apply the correspondence principle.

Let us now consider the development of the application of quantum theory to the superconducting state. Consideration of the

Meissner effect in superconductors led F. London (1) to propose that the local momentum, $p_s = mv_s + eA$, had a certain rigidity in superconductors. In 1948 (2) he extended this idea and proposed that the superconducting state be considered as a single macroscopic quantum mechanical system, by virtue of the long range order of the momentum vector. This long range order results from a kind of condensation into a quantum single state in momentum space. As a result of this idea he was led to the conclusion that within a superconductor $p_s = 0$, with the result that the supercurrents were directly related to the magnetic field. A more far reaching consequence, on applying the theory to a superconducting ring, was the prediction that the flux through such a ring obeyed the Wilson, Sommerfeld quantum condition, $\varphi = \frac{1}{q} \oint p_s ds = K\frac{h}{q}$ where K was an integer, and q the charge of the carriers.

A successful microscopic theory of superconductivity, produced by Bardeen, Cooper and Shriefer in 1957 (3), was based on just such a condensation in momentum space as London had visualized. This condensation was found to result from a pairing of the electrons at the Fermi surface. In 1961, London's prediction of flux quantization in a superconducting ring was verified for rings 10 to 20 μ in diameter (4, 5), and it was established that the appropriate value for q was the charge of a Cooper pair, 2e.

Recently, quantum tunneling of single electrons from a superconductor through a relatively thick oxide barrier has been used extensively to investigate the energy spectrum of superelectrons (6). A more subtle effect was first investigated theoretically by Josephson in 1962 (7). Josephson realized that those electrons which had undergone a Bose condensation to form the superconducting ground state of Cooper pairs could also tunnel,

as pairs, through sufficiently thin (about 10 Å) insulating layers separating coupled superconductors, and would do so without resistance. He in fact predicted two effects;

1. Cooper pairs can tunnel through barriers separating loosely coupled superconductors without energy loss (i. e., neither phonons or photons are created) to give a zero voltage supercurrent of maximum magnitude proportional to the ratio of the energy gap to the normal resistance of the insulating film. Considering the de Broglie wave nature of the electrons one can deduce that the amplitude of this tunneling (which depends sinusoidally upon the local phase difference of the wave functions across the barrier) should depend upon magnetic field, in analogy to the dependence upon path difference for light waves traversing a slit in classical Fraunhofer diffraction. The characteristic sin x/x behavior was first observed by Rowell (8) who found that indeed x was $2\pi B\, a/B_0 a$ as predicted (a is the effective area of the junction and $B_0 a = \varphi_0$, the quantum of flux).

2. An ordinary current will of course flow if a voltage difference is maintained between two loosely coupled superconductors. The energy difference, ΔE, associated with this voltage, has the additional effect on the coupled wave functions of contributing to the local phase difference a term $(t\Delta E/\hbar)$ causing the phase across the barrier to increase uniformly in time. The Josephson tunneling current, which now involves the tunneling of Cooper pairs with the emission of a photon of energy ΔE, is sinusoidal in the local phase difference and so alternates with a frequency of $2eV/h = 483.61$ MHz per μ V. Each cycle corresponds to the passage through the junction of one quantum of flux. Conservation of energy requires

that each Cooper pair transmitted through the barrier emit a photon of energy ΔE. The corresponding radiation has been detected directly (9). It has also been indirectly observed (10) as constant voltage steps in the I-V curve of single junctions when the frequency generated matches the electromagnetic resonant modes of the junction ("AC step structure"). These steps are attributed to the build up of relatively large r.f. fields in the junction which, by frequency modulation of the AC supercurrents, produce excess direct currents which give rise to the zero (or lowered) resistance structure in the I-V curve.

Both of the effects predicted by Josephson have recently been observed in numerous laboratories, and the technique is sufficiently well established that it may be used as a tool to study directly properties of the quantum mechanical wave function on a macroscopic scale.

The most critical test of the wave nature of a phenomenon is observation of the interference of coherent waves traversing different paths from a phase coherent source to the point of observation. Such de Broglie wave interference was observed by Mercereau et al., (11) for the zero-voltage quantum tunneling of superconducting electron pairs (Cooper pairs) through two Josephson junctions separated by 3.5 mm, and more recently (12) by 3 cm.

The initial object of the present work was to extend the range of observed phase coherence of the superconducting state wave function to lengths in excess of one meter ("the height of a small boy").

If phase coherence over such lengths was not observed a study of the breakdown of phase coherence at shorter lengths would be appropriate. If such macroscopic phase coherence were

observed, studies of propogation times in the quantum system were envisioned (about 3×10^{-9} sec/m at the velocity of light and 10^{-6} sec/m at the Fermi velocity), or if it seemed appropriate and interesting, extension to even longer lengths was to be considered.

Extensive effort in the early stages of the research was devoted to the development of techniques for reliably constructing Josephson interferometers. The major problems to be solved involved forming reliable junctions, insulating from each other the superconducting links connecting the junctions while maintaining desirable geometry, and making dependable electrical contacts to these superconducting links. The most successful technique (which is described more fully later) consisted of forming junctions by the controlled oxidation of a niobium substrate, covering all but the junction areas with a 1 μ Formvar sheet, and evaporated a convoluted tin strip connecting the junctions. Contact to the superconductors was made by attaching wires to the Formvar film with Indalloy solder which was arranged to contact one or the other superconductor.

Early experiments using interferometers with 4 cm superconducting links connecting the Josephson junctions (10 times the junction separation reported up to that time) were utilized to verify the operation and sensitivity of the detection system, to develop experimental familiarity with the phenomena associated with Josephson junctions and interferometers and to develop adequate magnetic and r.f. shielding. This shielding is critical, as even small stray r.f. fields seriously perturb the coupling of the quantum wave functions across the junctions. Furthermore, for the geometry of these experiments the magnetic field associated with one quantum of flux is 1 to 2 orders of magnitude less than fluctuations in the ambient magnetic field. These shielding problems were all solved

by operating inside a superconducting cylinder within a 1.7 meter long Mu-metal shield, and inserting low pass ($f_o \sim 6$ kHz) filters in each lead into the experimental region. An interferometer consisting of two Josephson junctions separated by a 0.8 meter superconducting link was then constructed and interference patterns (periodicity in amplitude of DC Josephson current versus applied magnetic field) were obtained, successfully demonstrating phase coherence of the superconducting wave functions over this truly macroscopic distance.

An interesting new effect was observed in an interferometer in which a 1.33 meter superconducting link connected the junctions. This interferometer showed no measurable (< 0.2 na) zero-voltage tunneling (no DC Josephson effect). However, detailed study of the I-V curve revealed a well developed step structure similar to that often obtained with single Josephson junctions. Such structure is generally attributed to resonant modes of the (typically 0.1 to 1 mm long) structure being excited by the AC Josephson effect. In this case, however, the voltage separation between steps corresponded to frequencies characteristic of the electromagnetic modes of the superconducting links connecting the junctions, treated as a transmission line. Observations of the interactions between the interferometer, the electrodynamic system, and the Josephson junctions were immediately undertaken and will be discussed later.

II. DESIGN CONSIDERATIONS AND DESCRIPTION OF APPARATUS

Our objective in the present section is to describe the various components of the experimental apparatus in light of their functions in this experiment. To this end the relevant design considerations are also presented. In several cases these considerations are dependent upon material discussed later in the thesis. In such cases forward references are made in order to allow a meaningful description of the experimental apparatus and techniques to be presented here.

A. Shielding

The maximum energy coupling the quantum phase of the condensed state wave functions across a Josephson junction of area σ supporting a tunneling current density j_1 will be shown to be (Equation 6)

$$\Delta E \text{ coupling} = \frac{h}{2e} j_1 \sigma \sim 2 \times 10^{-23} \text{ joules}$$

for typical tunneling currents (10^{-8} amps) observed in these experiments. It is consequently necessary to shield the experimental region against external perturbation to approximately this level. A further problem is that the oxide layers forming the junctions are very sensitive, being of the order of 10 Å thick, and are easily shorted, e. g., by switching transients or voltages induced by rapidly changing fields. Exceptional shielding against ambient magnetic field changes is required as interference periods of 0.3 mG were expected, orders of magnitude smaller than observed

fluctuations in ambient fields. Finally, r.f. interference from local sources and from commercial transmitters on Mt. Wilson is readily picked up (even on shielded, twisted pair leads) and conducted into the shielded experimental region producing "random" fields and voltages comparable to the desired effects.

Shielding against fluctuations in the ambient magnetic field was accomplished by placing the sample and the solenoid which produced the variable magnetic (interference) field inside a long superconducting cylinder. In order that this superconducting cylinder not trap a significant fraction of the earth's field when first cooled below its transition temperature, the entire dewar was placed inside a high permeability iron cylinder (Mu metal) which reduced the internal field to a few milligauss. This Mu metal shield also protected the experimental region from the direct influence of fluctuating fields over essentially the entire electromagnetic spectrum. By carefully shielding the external circuitry against low frequency AC signals (such as 60 Hz and 180 Hz from the power lines etc.) and placing low pass filters in each lead at the dewar cap to exclude radio frequency noise the sample was essentially isolated from external interference. The low pass filters used (Erie 1200-014) had 25 dB attenuation at 30 k Hz increasing to over 65 dB above 300 k Hz. Even at 6 k Hz the filters introduced 180^{o} phase shift requiring that signal frequencies less than 1000 Hz be used to obtain useful data.

B. Quantum Circuit

A de Broglie wave interferometer responds to the flux which it encloses. However, any finite inductive impedance in such a device will produce a self flux from the driving current, compli-

cating the response (see argument preceding Equation 20). In fact, if the inductive imbalance (ΔL) times the Josephson tunneling current is of order φ_0, ($\Delta L I_J = 2 \times 10^{-15}$ henry-amperes) the maximum Josephson current (which is dependent upon the total flux, applied plus self induced) becomes multiple valued and not reproducible (12). A primary design consideration in this experiment was therefore the fabrication of a low inductance interferometer circuit. As the inductance per meter of a feasible evaporated strip line is about 1/3000 that for any bifilar line, the two Josephson junctions were connected with a folded superconducting strip line.

This strip line consisted of a 1 mm wide tin strip 1300 Å thick (see Figure 1) evaporated onto a prepared niobium substrate (Nb) through a closely spaced mask. The substrate was prepared by carefully cleaning the niobium with a saturated solution of potassium dichromate in concentrated sulfuric acid ("cleaning solution") and rinsing it in distilled water and pure alcohol. The cleaned 2" x 3" niobium sheet was then dipped into a one percent solution of polyvinyl formal (7/95 - E Formvar) in p - Dioxane to a depth of 2-1/2" (leaving the region where the junctions were to be formed (C) clean) and removed slowly to form a thin uniform sheet of Formvar (D) which was allowed to harden for several hours. The sample was then dipped again into the Formvar solution, removed quickly, and placed flat in a slightly open petri dish containing saturated p - Dioxane vapors to dry and harden. This technique produced relatively uniform, pinhole free, insulating layers of Formvar 0.5 to 1.5 microns thick with fair reliability. Extra Formvar was added to thicken the contact areas (E) and #44 (50 μ) copper wires were attached by soldering to the Formvar film with Indalloy. Contacts (F) to the niobium were made by taking care to

break through the Formvar film and the niobium surface oxide, while contacts (G) to the (not yet evaporated) tin film were made very delicately resulting in over 2 megohm resistance between the two leads. These current leads were connected at the point midway between the junctions to preserve symmetry.

The tin film was now deposited on the insulated region by rapid vacuum evaporation at 300°K substrate temperature and 5×10^{-6} tor. A machined mask close to the substrate (less than 0.5 mm away) defined a folded strip line 1.33 meters long. Sections (H) of the strip about 1.5 cm long at each end of the mask were shielded during this evaporation to prevent the tin from shorting to the bare niobium in the region (C) left for forming the junctions.

The capacitance and dissipation of the resulting capacitor were measured and from these the parallel resistance of the insulation and the effective thickness of the insulating layer were calculated. A high parallel resistance (of order 10 to 100 K Ω) was desired in order that there be no possibility of shorts through the insulation which might form additional Josephson junctions in parallel with the experimental junctions. The possibility of such parallel junctions would have invalidated the experimental observation of long range coherence by providing alternate shorter paths. Knowledge of the thickness of the Formvar film was required in order that the conversion from magnetic field to enclosed flux (Equation 18 and following discussion) could be made. The thickness was also required in the determination of the propagation velocity (Equation 26) in the strip line. For the particular sample for which AC effects are reported, the results at 300°K are as follows.

$$C_s = 54 \text{ nf} \qquad D = 0.26 \qquad C_p = \frac{C_s}{1 + D^2} = 50.6 \text{ nf}$$

$$t_c = \frac{\epsilon_r \epsilon_v \ell w}{C_p} = 0.68 \mu \qquad R_p = \frac{1}{\omega C_p D} = 12 \text{ K}\Omega$$

where C_s = series capacitance

D = dissipation factor, this improves to order 0.02 at lower temperatures.

C_p = parallel capacitance

t_c = effective dielectric thickness from capacitance measurements

ϵ_r = tabulated dielectric constant of type E Formvar, 3.12 at 1000 Hz and 26°C

ϵ_v = free space permitivity

ℓ = length of film, 1.30 meters

w = width of film, 0.95 mm

R_p = parallel (leakage) resistance of insulating film

The thickness of the film was judged to be relatively uniform ($\pm$ 50%) by observing the interference fringes produced by fluorescent lights reflecting from the niobium sheet and from the film surface. In particular, no very thick or thin spots were noted. Reasonable

variations in thickness have little effect on the capacitance as can be seen by assuming a sinusoidal variation in thickness from the mean, of amplitude τ. Then,

$$\frac{C}{C_o} = \frac{t_o}{2\pi} \int_0^{2\pi} \frac{dx}{t_o - \tau \cos x} = \frac{1}{1 - \tau^2/t_o^2} \quad ;$$

and if

$$\tau/t_o \sim 0.5, \text{ then } t_{max}/t_{min} = 3 \text{ and } C/C_o = 1.15 .$$

Fortunately such uniform thickness variations have little or no effect on the area available for enclosing flux, i.e., in the inductance, as

$$\frac{1}{2\pi} \int_0^{2\pi} (t_o - \tau \cos x)\, dx = t_o \quad .$$

As the area of the interferometer exposed to externally generated flux (the effective area) is only about 0.03 mm^2, a single uncompensated "bubble" of insulator (or contaminant), e.g., extending over 1 mm and 10 μ thick, could alter the effective area by up to 30%. Care was taken to avoid such "bubbles" by operating under a dust free hood and keeping all solutions and materials meticulously clean. However, it is not possible to give absolute assurance that no such "bubbles" occurred over the 50 mm by 75 mm surface on which the interferometer was constructed.

After ascertaining that a usable film had been obtained, the sample was completed by forming the Josephson junctions. The "clean" end (C) of the niobium sheet was wiped with p - Dioxane and then stripped of oxide by a 30 second exposure to concentrated NaOH. The NaOH was wiped off with cotton swabs dipped in distilled water, alcohol, and finally swabs which had been refluxed for an hour in p - Dioxane. The clean niobium surface was allowed to oxidize for 17 hours in wet oxygen. Formvar solution was painted over the entire oxidized surface with the exception of regions (J) about 0.5 mm square located 1 cm from the ends of the previously evaporated tin film. After hardening for about two hours the sample was again placed in the evaporator and 1300 $\mathring{A}$ of tin was deposited through the entire area of the mask used to form the underlying capacitor strip, now including the junction area. Typical junction resistances obtained in this way were 5 ohms at $4^{o}K$.

C. Magnetic Field Assembly

It is necessary in the course of the experiment to produce a uniform magnetic field of a few tens of milligauss over the entire region occupied by the interferometer. This field must be essentially parallel to the surface of the niobium sheet carrying the interferometer, or field determinations will be confused by the demagnetizing effect of the niobium. Parallelism was assured by clamping the niobium sheet (Nb, Figure 2) carrying the completed interferometer to a 5.1 cm wide phenolic sheet (P) which was a slip fit into the solenoid winding cylinder (S). The solenoid was wound on a 5.4 cm OD by 0.15 cm wall phenolic cylinder which had been shallowly threaded 26 turns per inch (1.05 turns per mm). Epoxy

paint was used to hold the #22 Formvar coated copper wire in place over the 20 cm length of the winding. Field uniformity over the central 7.5 cm was significantly improved by over-winding 28 turns at the same pitch at each end. This assembly was supported from the dewar cap on three 0.45 cm diameter phenolic tubes and was assembled using nylon screws to preclude magnetic impurities (the twinax leads used in the dewar were all copper and teflon for the same reason).

To completely shield the sample from external fluctuating fields, this entire assembly was slipped into a 1 mm wall tin cylinder (Q) 6.1 cm ID and about 25 cm long. Tissue wrapping was used to assure coaxiality of the shield and field coil, while the phenolic plate carrying the sample was a tight slip fit inside the solenoid.

For a long solenoid the magnetic field calibration in free space, of course, is $\mu_0 NI$. However, this is drastically modified by the close fitting superconducting shield (Q) which maintains the flux through itself constant, nominally zero in this case. Thus, if r is the solenoid radius and R the inner radius of the tin shield, a current through the solenoid which would produce a uniform field, $B_{o'}$ within it will induce currents in the shield which would produce an opposing field, B', such that, neglecting the small return flux of the long solenoid,

$$\pi r^2 B_o = -\pi R^2 B' \quad .$$

The resulting field within the solenoid is approximately

$$B = B_o + B' = B_o \left(1 - \frac{r^2}{R^2}\right) = B_o \frac{1}{4.55} \quad .$$

This result was verified and the field uniformity measured by applying a 30 kHz drive to the solenoid and detecting the signal induced in a movable pick up coil inside it. It was found that with the tin cylinder at 77°K (where the skin depth at 30 kHz is about 0.15 mm), the signal decreased by a factor of 4.76 when the solenoid assembly was lowered into the tin cylinder. By moving the detector coil vertically it was possible to measure the field uniformity. With the number of overwound turns on each end adjusted to 28, the field with the assembly inside the magnetic shield was uniform to within one percent over the central 7.5 cm of the solenoid.

A final verification of the field attenuation factor was obtained when an interference pattern was obtained at 3.75°K (thin evaporated tin films usually have transition temperatures somewhat above the bulk transition temperature of tin at 3.72°K). This pattern was compared with the interference pattern obtained below 3.72°K. After making a 5% correction for the change in effective area of the interferometer due to the changing penetration depth of the tin film, a field ratio of 4.35 was obtained.

As each of these determinations carried errors of 5% or so the average of all the values (4.55) was used in calculating the actual magnetic field.

D. Classical Circuits (Electronics)

A major problem in this experiment is electrical interference with the sample from both line frequency and radio

frequencies. Such interference was minimized by operating all critical circuits balanced to ground, by using heavily shielded twisted-pair leads, and by enclosing the entire dewar in a Mu-metal shield.

Numerous techniques are available for observing the DC Josephson effect. The objective in general is to observe, as a function of applied magnetic field, the maximum value of the zero voltage current which tunnels between two superconductors coupled by Josephson junctions. If this current, supplied from an external source, is increased slowly from zero no voltage will appear between the superconductors until the maximum value of the Josephson current is reached. At this point the voltage will shift along the load line of the circuit to the appropriate point on the Giaever single particle tunneling characteristic and follow that curve until the current is returned to zero.

Because of its convenience and the availability of the required electronics a four terminal constant current AC (100 Hz) technique was chosen. In this technique (Figures 3 and 4) an alternating current (I) from an external high impedance source tunnels from one superconductor to the other through the Josephson junctions (J) and the instantaneous voltage (V) developed between the superconnectors is observed on independent terminals as a function of the instantaneous current. For example, a voltage proportional to the drive current may be used to provide X-axis deflection of an oscilloscope, and the amplified voltage appearing across the sample may be used to provide Y-axis deflection. In this way an I-V curve characteristic of the Josephson junctions may be observed on the oscilloscope; typical displays are shown in Figure 4. The DC Josephson current is taken as that point on the

I-V curve where a voltage is first developed across the junctions. In general, this point may be easily identified, as the voltage jumps from zero along the circuit load line to a value characteristic of the single particle tunneling curve of the junctions.

In the course of the experiments discussed in this thesis it was necessary to obtain detailed plots of the I-V curve of the interferometer and at other times to observe the behavior of the zero voltage Josephson current (I_J) with magnetic field. Because of the large superimposed noise signal associated with the 1000 Hz band width of the amplifier, the very low signal levels encountered in these experiments precluded observing either effect directly on an oscilloscope as described above. This signal to noise problem was resolved by resorting to a narrow band ($\Delta f \sim 0.1$ Hz) detection scheme employing a "lock-in amplifier" or "phase sensitive detector". The DC output signal of the phase sensitive detector (PSD) was plotted on an X-Y recorder while the independent variable was slowly varied over the range of interest in a time of the order 10 minutes. Utilizing the PSD, I-V curves were obtained indirectly by a derivative technique. The AC (100 Hz) current through the sample was set to a value small (typically 2.0 na) compared to the features of interest in the I-V curve. This constant 100 Hz probe current was used to modulate an adjustable DC bias current through the interferometer. As the DC bias current was swept through the interesting region of the I-V curve the DC voltage developed had superimposed upon it a varying 100 Hz voltage. The alternating voltage across the sample under these conditions was a measure of the incremental resistance (dV/dI) at the point on the I-V characteristic determined by the DC current through the sample. Plots of dV/dI versus I_{DC} were obtained by amplifying and phase

detecting the (small) AC signal and recording it on the X-Y recorder against (a voltage proportional to) the DC current through the sample while this current was slowly varied (see Figures 5, 7 and 8). The I-V characteristic was then reconstructed by manually integrating the dV/dI versus I_{DC} curve (see Figures 6 and 9).

Recordings indicating the magnetic field dependence of the zero voltage Josephson current were also obtained by use of the PSD. In this case an appropriate peak value for the (unbiased) 100 Hz current through the interferometer was chosen to exceed the maximum Josephson current observed on the integrated I-V plots. The amplified and phase detected signal was recorded on the X-Y recorder versus the current through the magnetic field coils as this current was slowly varied. The maximum value of the zero voltage Josephson current (I_c) is periodic in the (slowly changing) flux linking the interferometer. Hence, the time average of the voltage developed across the interferometer will show this same slow periodicity.

Assuming a linear I-V curve for voltages much less than the energy gap, the voltage (Figure 4) across the interferometer in each half cycle is just zero until I exceeds I_c, and $V = V_P \sin \omega t$ for the rest of the half cycle. A filter in the input stage of the PSD passes only the fundamental Fourier component of this waveform, which has amplitude

$$a_1 = \frac{2}{\pi} V_P \int_{\arcsin I_c/I_P}^{\pi} \sin \omega t \sin(\omega t + \alpha)\, d(\omega t)$$

$$= \frac{2V_P}{\pi} \left[\pi \cos\alpha - \sin\alpha \left(\frac{I_c}{I_P}\right)^2 + \cos\alpha \left(\frac{I_c}{I_P} \sqrt{1 - \frac{I_c^2}{I_P^2}} - \sin^{-1} \frac{I_c}{I_P} \right) \right] .$$

Choosing α (the phase shift added to the PSD reference voltage) to emphasize the lowest order variable term ($\alpha = \pi/2$) we note that the response is quadratic in I_c/I_P. As the periodicity with magnetic field is the feature of interest, the nonlinear nature of the effect is of no particular consequence. The interference patterns (Figures 10 and 11) were obtained in essentially this way.

A block diagram of the electronic system is shown in Figure 12. An oscillator (HP200CD shunted by a 10 Ω load) applies a 100 Hz voltage across the two 0.5 megohm resistors in series with the (low resistance) sample. The voltage across this 1.0 megohm is monitored on the X axis of an oscilloscope, and may be adjusted to set the current through the sample between 1 na and 1 μa. To improve the noise figure of the detection system and provide impedance matching a heavily shielded transformer (Triad G-4) with a 50:1 voltage step up ratio is placed directly across the sample. The transformer output is amplified by 1000 in a low noise differential preamplifier (Keithly 103) with a band width adjusted to 1000 Hz and a low frequency cut of 10 Hz. The single ended output signal is delivered to the Y axis of the oscilloscope upon which the I-V curve characteristic of the sample may be observed directly (along with considerable noise). It is also fed to a phase sensitive detector, "PSD", (EMC model RJB) which is referenced to the driving oscillator. A twin-T filter in the PSD narrows the band width to 5% to prevent overloading on noise pulses and to remove signals appearing at harmonics of the reference frequency.

Following the phase sensitive diode bridge (which coherently demodulates the signal) is an RC filter which determines the noise band width of the phase detected signal. Values of the RC time constant of 0.3 to 10 seconds were generally found desirable to minimize the noise without adversely affecting the system response time. The DC output of the PSD was delivered to a Moseley X-Y recorder (model 2D2). The magnetic field drive was provided by an H Labs (model 955B) power supply. The output voltage was fed through a 60 Hz RC filter and 1 kΩ, 10 kΩ or 100 kΩ resistor to a reversing switch and the field coil. The voltage across this resistor was delivered to the second axis of the X-Y recorder when interference patterns were being plotted. At such times the 855B power supply was used as a DC cathode follower supplied by an RC circuit with a time constant of 10 to 100 seconds. By this ruse the relatively large noise signal generated by adjusting potentiometers was avoided and smooth, clean field sweeps were achieved. To obtain I-V curves in the presence of the (relatively large) thermal noise voltage it was necessary to resort to a derivative technique. In this technique a variable DC bias current modulated by a small alternating current of constant amplitude was applied to the sample (Figure 12). The resulting (small) AC voltage was detected on a phase sensitive detector. The PSD output was plotted on the X-Y recorder against (a voltage proportional to) the DC bias current to provide dV/dI vs I_{DC} plots. The variable DC bias current was derived by turning (at 1 rpm) the tap of a 100 Ω, 10 turn, potentiometer carrying 1 ma of direct current. The voltage developed at the potentiometer tap was heavily filtered and introduced in series into the interferometer drive circuit. It was necessary to prevent the DC current applied to the sample from being bypassed through

the low DC resistance of the impedance matching transformer in the output circuit. A 500 μ fd - 3 volt electrolytic blocking capacitor was introduced into each lead of the transformer for this purpose. These capacitors also eliminated pattern asymmetries previously observed. These asymmetries had been attributed to a thermal EMF in the output circuit causing a current to circulate through the low resistance of the transformer and the sample.

III. DATA CHARACTERISTICS

The main features of the data obtained with the equipment described above will be mentioned briefly in this section. A detailed discussion will be held for later.

A. DC Josephson Effect

On some low resistance junctions (R_N = 40 m Ω) diffraction patterns indicating DC Josephson currents, (I_J), as large as 28 ma were observed. However, interference was never observed on any macroscopic interferometer with I_J > 15 na. Interference effects were observed on several samples. By sweeping the magnetic field at about 0.5 mg/min an interference pattern (variation of tunneling current with magnetic field, Figures 10 and 11) was obtained on the X-Y recorder at all temperatures below 3.8°K (T_c bulk tin - 3.72°K). Interference effects were observed for any setting of drive currents (AC or DC) within the range where dV/dI varied with I_{DC}. One interferometer with I_J = 12 na had a very well developed interference pattern (Figure 10) of the appropriate periodicity, demonstrating phase coherence of the de Broglie waves of the superconducting electrons over its length of 0.8 meters. No enhancement of the DC tunneling current was observed for any value of DC voltage across this sample, i.e., no "AC step structure" was observed.

B. AC Josephson Effect - Step Structure

It is shown in the appendix that the DC Josephson effect may average to zero in the presence of noise for junctions which are insufficiently coupled. However, a particularly well developed

structure of constant voltage steps was observed in the I-V curve (Figure 9) of one interferometer which showed no zero voltage Josephson current (< 0.2 na). For a given magnetic field, the steps were separated by about $1/4\ \mu$ v, corresponding to a Josephson frequency of about 120 MHz. Two orthogonal sets of modes were observed, with amplitudes showing the appropriate quantum periodicity in the magnetic flux linking the interferometer. This behavior can be predicted from analysis of the AC Josephson current in a resonant structure, such as the strip line formed by the superconducting arms of the interferometer. As these resonant modes are orthogonal to one another, it is possible to "tune" to one or the other mode by adjusting the magnetic flux. It thus appears that the presence of the superconducting cavity linking the two junctions has provided coherence between the thermally uncoupled superconductors.

IV. ANALYSIS

A. The Josephson Effect

In order to discuss in detail the experimental results reported in the previous section it is necessary to develop the theory of Josephson currents in considerable detail. In particular we must study the interaction of these currents with the superconducting circuit connecting the junctions under our experimental conditions. As a first step in this direction we will devote this section to sketching the quantum mechanical derivation of the Josephson current which flows between coupled superconductors.

Phase transformations, such as that to the superconducting state, are generally indicative of the transition of the system in question to a lower entropy configuration. Often this lowered entropy is achieved by the establishment of some kind of long range coherence. For example, the aligning of electron spins over macroscopic distances leads to the establishment of the ferromagnetic state having a permanent magnetic moment. The process occurring in the phase transition to the superconducting state is not so clearly seen on an intuitive level as the above classical example as it is entirely quantum mechanical in nature. The superconducting transition arises from a condensation of the conduction electrons into a single quantum mechanical ground state of electron pairs, each with identical momentum, $p = m^*v + e^*A$ (here m^* and e^* are the mass and charge of an electron pair). The coherence of the quantum wave function which results from this correlation of the pair momentum allows us to describe the state of order in the system in terms of a complex position-dependent order parameter, ψ. This order parameter has properties similar to those of

elementary quantum mechanical wave functions (13). Such wave functions have the property that their phase, $\gamma = \arg \psi$, and the number of particles (pairs), $N = \int \psi^* \psi \, d\,\text{vol.}$, are conjugate variables. As such they cannot both be specified with arbitrary accuracy, but obey an uncertainty relationship, $\Delta\gamma \, \Delta N = \hbar$ (14). Thus, if either N or γ is known precisely the other is indeterminate.

Experiments (such as the Meissner effect) tells us that within a single block of superconductor the relative phase is fixed rigidly; hence, there must be locally a coherent superposition of different N states. In contrast the value of N in each of two isolated blocks of superconductor is fixed, and the relative phase is meaningless. However, if two such blocks are connected by a thin insulating barrier the possibility of the tunneling of pairs through the barrier arises, leading to a situation intermediate between the two just discussed. The phase of the entire system is again meaningless, but the relative phases of the two blocks of superconductor are not meaningless. Pair tunneling leads to the possibility of numerous N states, the coherent superposition of which results in a lowering of the total system energy by virtue of the phase coupling across the barrier. Anderson (14) obtains an expression for the energy per unit area resulting from this coupling of the phases. He writes the second order energy perturbation resulting from the transition (by virtue of an exponentially small tunneling matrix element, T) of pairs from superconductor 1 to 2 at zero temperature as

$$\Delta\mathcal{E} \cong -N_1 N_2 \, \langle |T^2| \rangle 2\pi^2 \frac{\Delta_1 \Delta_2}{\Delta_1 + \Delta_2} \cos(\gamma_1 - \gamma_2) = \left(\frac{\Delta E}{t}\right) \cos(\gamma_1 - \gamma_2) \qquad (4$$

where ΔE is the coupling energy density per unit volume in the barrier (of thickness t) and Δ_1 and Δ_2 are the BCS energy gaps of the two superconductors. (The approximation is quite good if the ratio of energy gaps is less than about 3.).

Because this result depends on the phase difference, $\gamma_1 - \gamma_2$, of the order parameter across the barrier it is not gauge invariant. In the presence of a vector potential, gauge invariance is assured if the phase everywhere is modified by a term $2e/\hbar \int A \cdot d\ell$, where the integration follows a path always within the region of phase coherence from some arbitrary point to the place in question. Thus the energy which couples the phases of the order parameter across a barrier becomes

$$\Delta\mathcal{E} = \left(\frac{\Delta E}{t}\right) \cos\left(\gamma_2 - \gamma_1 - \frac{2e}{\hbar} \int_1^2 A \cdot d\ell\right) . \qquad (5$$

In quantum mechanics such a dependence of the energy on the vector potential implies a current flow. The density of this supercurrent which flows from point 1 to 2 (separated by the barrier of thickness t) is defined in terms of the Hamiltonian of the system, H, as

$$\langle J \rangle = \frac{\delta \langle H \rangle}{\delta A} = \frac{2e}{\hbar} \Delta E \sin\left(\gamma_2 - \gamma_1 - \frac{2e}{\hbar} \int_1^2 A \cdot d\ell\right). \qquad (6$$

Josephson (7) has defined $(2e/\hbar)\,\Delta E$ as j_1, $\langle J \rangle$ as j_z and pointed out that $(2e/\hbar)\, N_1 N_2 \langle T^2 \rangle\, 2\pi$ corresponds to the conductance $1/R_N$ of the barrier of area σ when the superconductors are both in the

normal state. The maximum zero voltage current which can flow through the barrier is thus equal to that which would flow if a voltage equal to $\pi\Delta_1\Delta_2/(\Delta_1 + \Delta_2)$ were impressed across the resistance R_N. Thus

$$j_z = j_1 \sin \delta(x,t) \qquad (7$$

where

$$j_1 = \frac{\pi \Delta_1 \Delta_2}{\Delta_1 + \Delta_2} \frac{1}{R_N \sigma}, \quad \delta(x,t) = \gamma_2 - \gamma_1 - \frac{2e}{\hbar} \int_1^2 A \cdot d\ell$$

and the Josephson current is sinusoidally related to the instantaneous, local, gauge invariant, phase difference across the barrier.

B. Phase Relationships

So far we have an expression for the Josephson current density in terms of the phase difference, δ, of the order parameter across the barrier, the phases being coupled by the energy ΔE. We wish to consider the interaction of this current with our superconducting circuit. However, it is first necessary to obtain expressions for the space and time variation of this phase difference in the presence of external fields and potentials.

The time variation of the phase difference can be written immediately for a quantum system in equilibrium. For such a system gauge invariance requires that we write $\psi(r,t) = \psi(r) \exp(-iEt/\hbar)$, otherwise simple changes of the reference from which we measure the energy, E, will change the time dependence

of ψ. With this explicitly time dependent form for ψ we can write a simple differential equation for the change in phase, $\delta(x, t)$, on crossing the barrier from superconductor 1 to 2, i. e.,

$$\frac{\partial}{\partial t}\,\delta(x,t) = \frac{\partial}{\partial t}(\arg \psi_2 - \arg \psi_1) = -\frac{E_2}{\hbar} + \frac{E_1}{\hbar} \ .$$

Now the energy associated with the transmission of a Cooper pair between two superconductors separated by a barrier supporting a potential difference, V, is 2 eV. Writing the energies in this form and integrating, we have the desired time variation in terms of the instantaneous voltage across the barrier

$$\delta(x,t) = \delta(x,o) - \frac{2e}{\hbar}\int V\,dt \ . \qquad (8$$

The spatial variation of the phase within a single piece of superconductor may be obtained directly from the Landau-Ginzburg expression for the current density

$$j = \frac{i\hbar}{2m}\,e(\psi \nabla\psi^* - \psi^* \nabla\psi) - \frac{2e^2}{m}\,\psi^*\psi A \ , \qquad (9$$

where 2e and 2m are the charge and mass of a Cooper pair. Operating with the gradiant on ψ^* and ψ, where ψ is of the form $\sqrt{N}$ exp (i arg ψ), the bracket gives - 2N grad (arg ψ). Integrating along a path entirely within a superconductor, the expression for the current can be rearranged to yield directly the spatial variation of the phase, i. e.,

$$\int_a^b \nabla(\arg \psi) \cdot d\ell = \arg \psi(b) - \arg \psi(a)$$

$$= \frac{2e}{\hbar} \int_a^b (A + \mu_o \lambda_L^2 j) \cdot d\ell = \frac{1}{\hbar} \int_a^b p \cdot d\ell = \int_a^b \frac{d\ell}{\lambda} \qquad (10$$

where $\lambda_L = (m/\mu_o e^2 2N)^{1/2}$ is the penetration depth, 2N is the number of paired electrons in the system, and $p = 2mv + 2eA$ is the momentum associated with the de Broglie wave length (λ) of the pairs.

In general, we will be interested in phase differences between points at the surface of thin superconducting films in an ambient field, $B_{||}$ (Figure 13). Screening currents flow on such surfaces so that j is not zero. In fact the surface current is $j_s = B_{||}/\mu_o\lambda$ where λ is the depth of penetration of the magnetic field, $\lambda = \int_o^\infty B \; dz/B_{||}$. As the screening current is proportional to the local field we have $j = j_s \, B/B_{||}$. Applying Gauss's law to a slice of superconductor (Figure 13) with a length of surface, y, exposed to a field $B_{||} = B \cdot \hat{j}$, we obtain the anticipated relation between the field and the surface current

$$B_{||} y = \oint B \cdot ds = \mu_o I = \mu_o y \int_o^\infty j \; dz$$

$$= \mu_o y \, j_s \int_o^\infty (B/B_{||}) \; dz = \mu_o j_s \lambda y \quad . \qquad (11$$

Thus, for a path just within the surface of a superconductor, where $j = j_s$, and writing λ_i for λ_L^2/λ, we have

$$\arg \psi(b) - \arg \psi(a) = \frac{2e}{\hbar} \int_a^b (A + \lambda_i B_{\parallel}) \cdot d\ell \quad . \tag{12}$$

We now wish to write the phase difference across the barrier (Figure 14a) at the point x, $[\delta(x, t)]$ in terms of the phase difference at an arbitrary reference point, $\delta(0, t)$. Referring to Equation 5, and recalling that $\gamma = \arg \psi$ we have immediately

$$\delta(x, t) = [\arg \psi_2(x) - \arg \psi_1(x) - \frac{2e}{\hbar} \int_1^2 A(x) \cdot d\ell]$$

$$+ \delta(0, t) - [\arg \psi_2(0) - \arg \psi_1(0) - \frac{2e}{\hbar} \int_1^2 A(0) \cdot d\ell]$$

$$= \delta(0, t) + [\arg \psi_2(x) - \arg \psi_2(0)] - [\arg \psi_1(x) - \arg \psi_1(0)]$$

$$- \frac{2e}{\hbar} \int_1^2 A(x) \cdot d\ell + \frac{2e}{\hbar} \int_1^2 A(0) \cdot d\ell \quad .$$

Replacing the square brackets by use of Equation 12 and combining the integrals on A we have

$$\delta(x,t) = \delta(0,t) + \frac{2e}{\hbar} \oint_{\Gamma} A \cdot d\ell + \frac{2e}{\hbar} \int_{o}^{x} (\lambda_1 + \lambda_2) B_{\|} \, dx$$

$$= \delta(0,0) - \frac{2e}{\hbar} \int V \, dt + \frac{2e}{\hbar} \int_{o}^{x} B_{\|} \, d \, dx \quad . \tag{13}$$

Here we observe that $\oint_{\Gamma} A \cdot d\ell = \int_{o}^{x} B_{\|} \, t \, dx$ (the flux in the insulator) where Γ indicates a path following the superconductor - insulator interface (dashed rectangle in Figure 14a). We have also found it convenient to define $d = t + \lambda_1 + \lambda_2$, the effective thickness of the flux sheet linking the junctions.

With a complete expression for the phase difference across a Josephson barrier, we are now in a position to obtain the zero voltage Josephson current transmitted by such a barrier in the presence of a uniform magnetic field, $B_{\|}$. Integrating the current density $j_z = j_1 \sin \delta$ over the area, $\sigma = XY$ of the barrier, we obtain

$$I = \int_{o}^{Y} dy \int_{-X/2}^{X/2} j_1 \sin\left\{\delta(0,t) + \frac{2e}{\hbar} \, d \, B_{\|} \, x\right\} dx$$

$$= \frac{(j_1 \, Y X)}{2(X/2)} \, \frac{\cos\left\{\delta(0,t) + \frac{2e}{\hbar} \, d \, B_{\|} \, x\right\} \Big|_{-X/2}^{X/2}}{(2e/\hbar) \, B_{\|} \, d}$$

$$= i_1 \, \frac{\sin(\pi\varphi_J/\varphi_o)}{(\pi\varphi_J/\varphi_o)} \sin \delta(0,t) \tag{14}$$

where φ_o is written for the quantum of flux, $\hbar/2e = 2.07 \times 10^{-15}$ webers; $\varphi_J = (X\ d)B_{\|}$ is the flux enclosed in the effective area of the junction; and $i_1 = j_1 \sigma$. In performing the integration a uniform j_1 was assumed. Small variations from uniformity act primarily to reduce the depth of the minima of the diffraction pattern, changing the cusp like pattern predicted above (see also Equation 21) to a more sinusoidal pattern. Although such effects have been observed they are of no particular significance in the work reported here and so will be neglected.

The above expression is analogous to that obtained for the amplitude in the Fraunhofer diffraction of light by a single slit. This analogy is reasonable if one adopts the viewpoint the electrons "actually" travel through the barrier as a de Broglie wave, the phase of which depends upon the ambient vector potential.

The phase difference $\delta(0, t)$ is determined by the circuit which drives the current through the junction. It will adjust from zero to $\pm \pi/2$ as the zero voltage tunneling current is increased from zero to its maximum value. The maximum zero voltage current which the junction will carry is determined by the magnetic flux linking the junction, and, of course, by i_1, which is related to the tightness of coupling of the two superconductors. If the maximum zero voltage tunneling current is exceeded, a voltage appears across the junction characteristic of the single particle tunneling curve (6). The superimposed Josephson current now alternates in direction as the term $\sin \delta(0, t) \rightarrow \sin \left(\pm \frac{\pi}{2} + \frac{2e}{\hbar} \int V\ dt \right)$ fluctuates with time; this is the AC Josephson effect for a single junction. Both the DC and the AC Josephson effect have been widely observed; the observations in general provide detailed confirmation of the theory and emphasize the quantum nature of the superconducting state.

C. Interferometer Phase and Current

Continuing the analogy between light waves and de Broglie waves one is led to consider the equivalent of the two slit optical interferometer. The physical realization of a quantum mechanical "de Broglie wave interferometer" consists of a superconducting loop broken by two Josephson barriers (Figure 14b). Current from an external source is caused to flow from one superconductor to the other, and the resulting voltage is observed by an appropriate detector. The current (I) through the device may be written as the sum of the currents through the two Josephson barriers, thus:

$$I = \left[\int dy \int j_1(x) \sin \delta(x,t)\, dx\right]_a + \left[\int dy \int j_1(x) \sin \delta(x,t)\, dx\right]_b . \tag{15}$$

In order to integrate this expression we use Equation 13 to expand the phase differences, $\delta(x,t)$, in terms of the phases at the reference points a and b centered in the two barriers, i.e., $\delta(a,t)$ and $\delta(b,t)$. Assuming the current density and magnetic field are uniform over the barriers we can integrate this expression, as before, to obtain

$$I = \left\{ \frac{\langle j_1\rangle_a\, Y_a\, X_a/2}{\frac{2e}{\hbar} B_{\|}\, d\, X_a/2} \cos[\delta(a,t) + \frac{2e}{\hbar} B_{\|}\, d\,(x-a)]\Big|_{a - X_a/2}^{a + X_a/2} \right\} + \{\quad\}_b$$

$$= \langle j_1\rangle_a\, Y_a\, X_a\, \frac{\sin \frac{2e}{\hbar} B_{\|}\, d\, X_a/2}{\frac{2e}{\hbar} B_{\|}\, d\, X_a/2} \sin \delta(a,t) + \{\quad\}_b$$

$$= I_a \sin \delta(a,t) + I_b \sin \delta(b,t) \quad . \tag{16}$$

Here the curly brackets indicate an identical expression with b substituted for a, Y_a and X_a are the dimensions of the junctions parallel and perpendicular to the applied field, and the diffraction effects are included in the current $I_a(B) = I_a$.

The interference effects resulting from the addition of these two sinusoidal currents are explicitly exposed by combining them through use of trigonometric identities. First, however, we need identical coefficients for the two sine terms. Writing Equation 16 in this way and proceeding we have

$$I = (I_a + I_b)\left[\frac{1}{2}\sin\delta(a,t) + \frac{1}{2}\sin\delta(b,t)\right]$$

$$+ (I_a - I_b)\left[\frac{1}{2}\sin\delta(a,t) - \frac{1}{2}\sin\delta(b,t)\right]$$

$$= I_T \cos\frac{\delta(a,t) - \delta(b,t)}{2} \sin\frac{\delta(a,t) + \delta(b,t)}{2}$$

$$+ I_c \sin\frac{\delta(a,t) - \delta(b,t)}{2} \cos\frac{\delta(a,t) + \delta(b,t)}{2} \tag{17}$$

where I_T is the current (including diffractive effects) transmitted by the interferometer, $I_a + I_b$; and I_c is the circulating current $I_a - I_b$. This expression may be written in a more useful form by combining the arguments after rewriting the phase differences at a and b by use of Equations 8 and 13. We need

$$\frac{1}{2}\left[\delta(a,t) \pm \delta(b,t)\right] = \frac{1}{2}\left[\delta(a,0) - \frac{2e}{\hbar}\int (V_2(a,t) - V_1(a,t))dt\right]$$

$$\pm \frac{1}{2}\left[\delta(b,0) - \frac{2e}{\hbar}\int (V_2(b,t) - V_1(b,t))dt\right]$$

$$= \frac{1}{2}\left[\delta_o + \frac{2e}{\hbar}\int_o^{\ell/2} B_{\|}\, D\, d\ell - \frac{2e}{\hbar}\int V(a,t)\, dt\right]$$

$$\pm \frac{1}{2}\left[\delta_o - \frac{2e}{\hbar}\int_o^{\ell/2} B_{\|}\, D\, d\ell - \frac{2e}{\hbar}\int V(b,t)\, dt\right] \qquad (18$$

where $\delta_o = \delta(0,0)$, $D = T + \lambda_1 + \lambda_2$ (T is the thickness of the Formvar sheet separating the superconducting strips of length ℓ), and $V = V_2 - V_1$. Inserting the appropriate expansion, and noting that $\frac{e}{\hbar}\int_{-\ell/2}^{\ell/2} B_{\|}\, D\, d\ell = \pi\varphi_I/\varphi_o$ where φ_I is the flux linking the interferometer, the current may now be written

$$I = I_T \cos\left[\pi\varphi_I/\varphi_o - \frac{2c}{\hbar}\int \frac{V(a,t) - V(b,t)}{2}\, dt\right]$$

$$\times \sin\left[\delta_o - \frac{2e}{\hbar}\int \frac{V(a,t) + V(b,t)}{2}\, dt\right]$$

$$+ I_c \sin[\pi\varphi_I/\varphi_o - \ldots] \cos[\delta_o - \ldots] \qquad (19$$

We wish to consider the behavior of the quantum circuit under several conditions of applied voltage and field, and so will refer frequently to this equation for the behavior of the quantum current in a de Broglie wave interferometer.

We will first consider briefly the effect of the circulating currents and residual inductive impedance on the behavior of the ideal interferometer. After studying such an ideal interferometer in the case of no applied voltage we will investigate its behavior under an applied steady voltage. The effects of the interaction of the resulting r.f. voltages generated from junctions (the AC Josephson effect) with the resonant cavity formed by the connecting superconductors will be considered in some detail. Finally, we will consider the disruptive effects of noise on the interferometer and see how this resonant cavity can induce phase coherence in a thermally decoupled ("normal") interferometer.

D. DC Interferometer

Circulating currents in an interferometer produce self generated magnetic fields which add to the applied field. If the flux produced by these currents is an appreciable fraction of a quantum unit, I_c and $B_{\|}$ become interdependent. As they are not monotonically related in Equation 19 we can expect that the critical value of the transmitted current may become a multiple valued function of the applied field. Such effects have been observed in numerous samples. The maximum value of the zero voltage Josephson current attains different values on subsequent trials, sometimes showing two or three relatively stable levels and sometimes having

a whole range of critical values. As it was not possible to obtain any useful interference curves or I-V curves with samples showing such instabilities we will not consider this subject further.

In an ideal interferometer the circulating current is zero ($I_a \equiv I_b$, i.e., the junctions are identical). Furthermore, the device is assembled so that the inductive impedance is as small as possible. This is accomplished by constructing the two arms (a and b) of the interferometer symmetrically and by making the enclosed area ($D\ell$) as small as feasible. To the extent these precautions are successful the flux linking the device is just that from the applied magnetic field. The response of the interferometer with zero applied voltage is then

$$I = I_T \cos(\pi \varphi \text{ (applied)}/\varphi_o) \sin \delta_o \quad . \tag{20}$$

If an external current source is connected to the interferometer the residual phase difference between the two superconductors, δ_o, adjusts between $-\pi/2$ and $+\pi/2$ to permit the current to flow. The maximum zero voltage current for which this adjustment occurs is

$$I_{max} = |I_T \cos \pi \varphi \text{ (applied)}/\varphi_o| \quad . \tag{21}$$

If the values of I_{max} are recorded as the flux is slowly varied, the interference pattern can be plotted out within the diffractive envelope, I_T. In our experiments (as discussed earlier) a high impedance (current) source of alternating voltage was used. In

this case a series of I-V curves is obtained as the flux is changed, and the values of I_{max} can be obtained from these. An interference pattern obtained on an interferometer 0.8 m long is shown in Figure 5.

E. AC Josephson Effect

If a current in excess of I_{max} is driven through the interferometer δ_o becomes $\pm \pi/2$ and a voltage appears across the barrier. In the absence of other effects this steady voltage is characteristic of the Giaever single-particle tunneling I-V curve of the junctions at the applied current. In addition to the single-particle tunneling, Josephson currents can still flow. It is clear that with an applied steady voltage (V) the phase of the sine term modulating I_T will increase continuously, causing the Josephson current to reverse in direction with a frequency $2e/h = 483.61$ MHz/μv. This constitutes the AC Josephson current which is superimposed on the steady single-particle current. This r.f. current is not generally observable in the external circuit, the capacity of the junctions, leads etc. shorts it out. However, the junctions do act as r.f. current sources which produce (small) r.f. voltages across the resistance of the junctions. At certain steady voltages the Josephson frequency matches a resonant frequency of the strip line formed by the superconducting links connecting the two junctions. At these frequencies resonant enhancement occurs and relatively large r.f. voltages appear at the junctions. Of course, it is clear that the r.f. voltage inducing resonances in the strip line need not result from the AC Josephson effect but could as well be externally supplied.

To study these effects we will assume the absolute magnitude of the superimposed r.f. voltage (v) is the same at a and b (by symmetry). However, the phase of the voltage at a and b may very well be different. In fact, we expect the phase difference ($\beta\ell$)to increase with frequency by π radians for each additional half wave length in the strip line. Thus, we assume

$$V(a,t) = V + v\cos(\omega t + \beta\ell/2) \text{ and } V(b,t) = V + v\cos(\omega t - \beta\ell/2) \qquad (22$$

substituting into Equation 19, writing $\alpha = 2ev/\hbar\omega$ and $\Omega = 2eV/\hbar$, and integrating, the transmitted current term becomes

$$\frac{I}{I_T} = \cos\left[\pi\varphi_I/\varphi_o - \alpha\,\frac{\sin(\omega t + \beta\ell/2) - \sin(\omega t - \beta\ell/2)}{2}\right]$$

$$\times \cos\left[-\Omega t - \alpha\,\frac{\sin(\omega t + \beta\ell/2) + \sin(\omega t - \beta\ell/2)}{2}\right] . \qquad (23$$

Equations of this form are known to have DC components whenever $\Omega = N\omega$. We can extract the DC component most simply by expanding the product into a sum of cosines and integrating over t, after making the substitution $t' = t \pm \beta\ell/2\omega$ as needed. This all gives

$$\frac{I_{DC}}{I_T} = \frac{1}{2}\left\{\frac{\omega}{\pi}\int_o^{\pi/\omega}\cos\left[\left(\pi\varphi_I/\varphi_o + \frac{\Omega}{\omega}\frac{\beta\ell}{2}\right) - (\Omega t' + \alpha\sin\omega t')\right]dt'\right.$$

$$\left. + \frac{\omega}{\pi}\int_o^{\pi/\omega}\cos\left[\left(\pi\varphi_I/\varphi_o + \frac{\Omega}{\omega}\frac{\beta\ell}{2}\right) + (\Omega t' + \alpha\sin\omega t')\right]dt'\right\} . \qquad (24$$

Combining the cosines by the half angle formula and removing the constant term from the integral, this becomes

$$\frac{I_{DC}}{I_T} = \cos(\pi\varphi_I/\varphi_o + \frac{\Omega}{\omega}\frac{\beta\ell}{2})\,\frac{1}{\pi}\int_o^{\pi/\omega}\cos(\Omega t' + \alpha\sin\omega t')d(\omega t')$$

$$= \cos(\pi\varphi_I/\varphi_o + \frac{\Omega}{\omega}\frac{\beta\ell}{2})\cdot J_{-N}(\frac{2ev}{\hbar\omega}) \qquad (25$$

where $N = 2eV/\hbar\omega = \Omega/\omega$.

Similarly $\frac{I_{DC}}{I_C} = \sin(\frac{\pi\varphi_I}{\varphi_o} + \frac{\Omega}{\omega}\frac{\beta\ell}{2})\cdot J_{-N}(\frac{2ev}{\hbar\omega})$.

This equation gives explicitly the time independent supercurrent flowing in response to a steady voltage, V, in the presence of an r.f. voltage, v sin ωt. This equation has several interesting features, whether the r.f. voltage is self-generated through the AC Josephson effect ($N \equiv 1$) or whether it results from external stimulation of the circuit. The amplitude of the interference term is now modulated by $J_{-N}(2ev/\hbar\omega) \sim (ev/\hbar\omega)^N - \ldots$, it is thus strongly dependent upon the magnitude of the r.f. voltage at the junctions. We will return to Equation 25 after a detailed study of the behavior of electromagnetic fields and voltages in the structure comprising an interferometer when this structure is considered as a transmission line.

F. Transmission Line Analysis

In addition to their quantum properties the interferometers developed in this research have interesting electromagnetic

properties. In order to interpret the experimental results it is first necessary to investigate the properties of the superconducting strip transmission line formed by the superconducting links which connect the Josephson junctions. Losses in such a line can be very small: the loss factor of the dielectric is typically reduced by an order of magnitude by the low temperature, while losses in the conductors are restricted to the penetration region, orders of magnitude smaller than the skin depth at microwave frequencies. The approximation of an ideal transmission line is thus quite good. For an ideal superconducting strip transmission line the velocity of propagation is

$$\frac{\omega}{\beta} = v_p = \lambda\omega/2\pi = \frac{1}{\sqrt{L'C'}} = \frac{c}{\sqrt{\epsilon_r}} \sqrt{\frac{T}{T + \lambda_1 + \lambda_2}} \quad . \tag{26}$$

For a superconducting strip line (width, w; separation, T) the capacity per meter is $C' = \epsilon_r \epsilon_v w/T$ while the inductance per meter is $L' = \mu_r \mu_v (T + \lambda_1 + \lambda_2)/w$. The inductance is increased by the depth of penetration of the magnetic field into the superconducting boundaries, $\lambda_1 + \lambda_2$, while the electric field does not penetrate the superconductors.

At frequencies such that the electromagnetic wavelength (λ) in the strip line is properly related to the length of the line (ℓ) impedance resonances will occur. For an "open" line for example, there is a set of "even" resonant modes corresponding to the voltage at the ends of the line being in phase and an "odd" set corresponding to their being out of phase. This phase difference between resonant maxima is given by $\beta\ell = n\pi = \frac{2\ell}{\lambda}\pi$ where $\beta\ell$ is the phase of the r.f.

voltage in Equation 22, and n is "even" or "odd". Whether the line is "open" or "shorted" is determined by comparing the terminating impedance, Z, with the characteristic impedance of the line, Z_o. By definition

$$Z_o = \sqrt{\frac{L'}{C'}} = \sqrt{\frac{T(T + \lambda_1 + \lambda_2)}{w^2} \frac{\mu_v}{\epsilon_r \epsilon_v}} . \qquad (27$$

In our case the line is terminated at each end by a current source ($I \sin\theta_i$) in parallel with the junction capacitance (c) and parallel resistance (R). The terms $\sin\theta_i$ are included to represent the relative phases of the two current sources. The equivalent termination is a voltage generator $Z_j I \sin\theta$ and an impedance $Z_j = R/(1 + \omega cR)$ connected in series across the line. For the junctions we are considering (~ 15 Å thick and 1/2 mm square) c is about 4nf and R is about 10 Ω. For the value of Z_o typical of our strip line, ($Z_o \approx 18\,\Omega$), the transition from "open" to "shorted" occurs at about 250 MHz.

Applying the general transmission line analysis to this situation, the voltage at the ends of the line may be written

$$v_i = \frac{Z_j I [\sin\theta_i - \sin\theta_j (\cosh\gamma\ell + \frac{Z_j}{Z_o} \sinh\gamma\ell)]}{(1 + \frac{Z_j^2}{Z_o^2}) \sinh\gamma\ell + \frac{2Z_j}{Z_o} \cosh\gamma\ell} \qquad (28$$

where θ is the phase of the current source. We write $\alpha + j\beta$ for the propagation constant, γ; $Z_o/R + j\omega c Z_o$ for Z_o/Z_j; and expand the resonance denominator into real and imaginary parts. After dropping higher order terms in Z_o/R and α we obtain

$$v_i = \frac{-Z_o I\left\{\sin\theta_i - \sin\theta_j\left[\cos\beta\ell + \frac{1}{\xi}\sin\beta\ell + j\left(\alpha\ell\sin\beta\ell - \frac{\alpha\ell}{\xi}\cos\beta\ell + \frac{Z_o}{R\xi}\sin\beta\ell\right)\right]\right\}}{\left[\frac{\xi^2-1}{2\xi}\sin\beta\ell - \cos\beta\ell\right] - j\left[\alpha\ell\,\frac{\xi^2-1}{2\xi}\cos\beta\ell + \left(\alpha\ell + \frac{Z_o}{R}\,\frac{\xi^2+1}{2}\right)\sin\beta\ell\right]} \qquad (29$$

where we have written ξ for $\omega c Z_o$. The approximation is quite good as we will find $Z_o/R \leq .03$ and $\alpha\ell \sim .002\ \omega/\omega_o$. The condition for resonance (real part of the denominator set equal to zero) is

$$\tan\beta\ell = \frac{2\xi}{\xi^2-1}\left\{\frac{1 + \frac{\alpha\ell Z_o}{R\xi^2}}{1 + \frac{2\alpha\ell Z_o}{R(\xi^2-1)}}\right\} \approx \frac{2\xi}{\xi^2-1} \qquad (30$$

where the terms in $\alpha\ell Z_o/R$ have been written primarily to indicate the validity of the approximations. Very near $\xi = 1$ it is necessary to consider the bracketed term since it tends to zero as ξ approaches one. In this region we have $\tan\beta\ell \sim \xi\,(R/Z_o)(1/\alpha\ell) \sim 1 \times 30 \times 100$, which is sufficiently large that $\beta\ell$ is not significantly changed from the value obtained using $2\xi/(\xi^2 - 1)$. Recalling that $\beta\ell = \pi\frac{2\ell}{\lambda} = \pi\frac{\omega}{\omega_o}$, we can solve Equation 30 iteratively for the resonance condition. Starting from $\xi = \omega c Z_o \sim .2\ n$, we find that below 300 MHz

$\beta\ell \sim .90\ n\pi$ while above 250 MHz $\beta\ell \sim (n - 1/2)\pi$; or in general $\beta\ell = \pi\, g(n)$. Thus the transition from "open" to "shorted" behavior is orderly, the phase slipping by about 20^{o} per resonant peak.

In order to determine the amplitude of the r.f. voltage at the resonances we use expression 30 for $\tan \beta\ell$ to reduce Equation 28; actually we use

$$\cos \beta\ell = [1 + \tan^2 \beta\ell]^{-1/2} = (-1)^n \frac{\xi^2 - 1}{\xi^2 + 1} \qquad (31$$

and $$\sin \beta\ell = \cos \beta\ell \tan \beta\ell = (-1)^n \frac{2\xi}{\xi^2 + 1} \ .$$

With this substitution the expression for the r.f. voltage in the line at resonance (v_r) reduces to the surprisingly simple result

$$v_r = \frac{-Z_o I_1 \sin \theta_j}{\omega^2 c^2 Z_o^{\ 2} + 1} - j \frac{Z_o I_1 (\sin \theta_j + (-1)^n \sin \theta_i)}{(1/\omega c Z_o)\left[\frac{2Z_o}{R} + \alpha\ell(\omega^2 c^2 Z_o^{\ 2} + 1)\right]} \qquad (32$$

where $(-1)^n$ is necessary to properly account for the arbitrary sign of the square root in the trig identity defining $\cos \beta\ell$; n is the number of the resonance peak. At resonance the real term is always small compared to the resonant term so we may neglect it.

G. Self Generated Effects

In the previous section we have considered the interaction between AC Josephson current flowing through resistive junctions and the electromagnetic resonant modes of the strip line connecting these junctions. The r.f. voltage self generated by the AC Josephson current at the strip line resonances is shown to be (Equation 32)

$$v_r = -j \frac{Z_o I_1 (\sin\theta_j + (-1)^n \sin\theta_i)}{\frac{1}{\omega c Z_o} \left(\frac{2Z_o}{R} + \alpha\ell (1 + \omega^2 c^2 Z_o^2) \right)} \qquad (33$$

where n is the number of the resonance peak ($n = V/V_o$ where at V_o, $\lambda = 2\ell$).

Let us first consider the resonant denominator in Equation 33. The term $2Z_o/R$ represents resistive loss in the Josephson junctions themselves. Exclusion of electromagnetic fields from the interiors of the superconductors and the relatively small conductivity of the normal component of electrons reduces losses in the conductors to negligible levels except for very near the transition temperature. Thus, except for the possibility of radiation, the attenuation in the superconducting strip line is primarily due to losses in the dielectric, $\alpha_d = Z_o G/2$ where G is the leakage conductance, $\sigma w/T$. The conductivity of a dielectric is $\sigma = \omega\epsilon_v \text{ Imag } \epsilon_r = \omega\epsilon \tan\delta$. Combining these expressions we have immediately

$$\alpha_d \ell = Z_o \frac{w\ell\omega\epsilon \tan\delta}{T} \; . \qquad (34$$

The more interesting behavior of Equation 33 is contained in the part $I_1(\sin\theta_j + (-1)^n \sin\theta_i)$. The resemblance of this expression to Equation 16 is not accidental, they in fact arise from the same considerations. The factor $(-1)^n$ is the only difference; it appears since the proper handling of signum ($\cos \beta\ell$, $\sin \beta\ell$) in the transmission line analysis has accounted explicitly for the phase factor δ_o implicit in Equation 16. To obtain detailed expressions for the phases θ_i and θ_j we reconsider Equation 19. Now, however, we are not interested only in the externally observable transmitted current ($I_a = I_b$), but must also consider the case $I_a = -I_b$. This represents a non-observable circulating current in the interferometer which, however, can also produce voltages at the junctions and thereby drive the electromagnetic modes of the strip line. Rewriting each term of Equation 19 as a sum of sines and ignoring the r.f. voltage terms we have

$$I = \frac{1}{2} I_T \left[-\sin(\Omega t - \delta_o - \pi \varphi_I/\varphi_o) - \sin(\Omega t - \delta_o + \pi \varphi_I/\varphi_o)\right]$$

$$+ \frac{1}{2} I_c \left[-\sin(\Omega t - \delta_o - \pi\varphi_I/\varphi_o) + \sin(\Omega t - \delta_o + \pi \varphi_I/\varphi_o)\right] .$$

Now

$$I_1 = \left\{ |I_c| \text{ when } \varphi_I/(\varphi_o/2) \text{ is odd}\right\} = \left\{ |I_T| \text{ when } \varphi_I/(\varphi_o/2) \text{ is even}\right\} ,$$

hence, we can rewrite this expression in the form

$$I = -\frac{1}{2} I_1 \left[\sin\left(\Omega t - \frac{m\pi}{2} - \delta_o\right) + (-1)^n \sin\left(\Omega t + \frac{m\pi}{2} - \delta_o\right)\right] \qquad (35$$

where $m = \varphi_I/(\varphi_o/2)$ and $\Omega = \omega_o \beta\ell/\pi = \omega_o g(n)$. This is identical in form to Equation 33 and we have explicitly identified θ_i and θ_j. Now let $\delta_o = \pm \pi/2$ (as it will if $\Omega \neq 0$), write $\sin[x - (\pm \pi/2)]$ $= \mp \cos x$, expand the cosines and combine to obtain

$$I = \pm I_1 \begin{cases} \cos\Omega t \cos m\pi/2 & (n \text{ even}) \\ \sin\Omega t \sin m\pi/2 & (n \text{ odd}) \end{cases} . \qquad (36$$

This replaces $I_1 (\sin\theta_i + (-1)^n \sin\theta_j)$ in Equation 33. This expression now explicitly demonstrates two independent sets of voltage resonances. The even (r.f. voltage in phase) modes are excited only when m is even, i.e., $\varphi_I = m\,\varphi_o/2 = k\,\varphi_o$; the odd (r.f. voltage out of phase) modes are excited only when m is odd, i.e., $\varphi_I = m\,\varphi_o/2 = (k + 1/2)\varphi_o$. We now substitute Equation 36 into Equation 33, write α as α_d using Equation 34, and replace v in Equation 25 with v_r (Equation 33). This gives explicitly the excess DC current self generated (N = 1) through the AC Josephson effect at the strip line resonances,

$$\frac{I_{DC}^{\text{resonant}}}{I_1} = \pm J_1 \left\{ \frac{2e}{\hbar} \frac{c\,Z_o\,I_1 \begin{cases} \cos m\,\pi/2 & n \text{ even} \\ \sin m\,\pi/2 & n \text{ odd} \end{cases}}{\frac{2}{R} + \frac{w\ell\omega\varepsilon \tan\delta}{2T}(1 + \omega^2 c^2 Z_o^2)} \right\} \times \cos(m\pi/2 + \beta\ell/2) \qquad (37$$

where we have shown in the previous section that at the n^{th} resonance of the strip line,

$$\beta\ell = \left\{ \begin{array}{ll} .9n\pi & n \leqslant 5 \\ (n - 1/2)\pi & n \geqslant 5 \end{array} \right\} = g(n)\pi \ . \qquad (38$$

As $J_1(x) \sim x/2$ for small x, the excess DC current will have resonant maxima as indicated whenever n and m have the same parity, and minima if different. Phase correlation between the quantum and the electromagnetic systems arises through the interaction, at the interface between the junctions and the strip line, of the Josephson currents and the electromagnetic field. If the flux linking the interferometer is integral the phase of the Josephson current is constrained by the quantum system to be the same at the two junctions. Under these conditions the Josephson currents will develop alternating voltages across the junction resistances (and across the ends of the strip line) which will be in phase. These voltages will selectively excite modes of the strip line having in phase voltages at the ends. Thus, if the Josephson frequency corresponds to a resonant mode of the strip line having in phase voltages at the ends, this mode will be excited by the Josephson current and resonantly enhanced by the strip line. An excess direct current results from the frequency modulation of the AC Josephson current by this coherent r.f. voltage. (If the flux linking the interferometer is half integral substitute out of phase for the same phase or in phase in the above argument.) The alternation of modes predicted by Equation 37 was observed through the excess direct current at all temperatures below T_c for n = 1 to

27 (57 to 1500 MHz) and m = ± 400 (± 200 flux quanta). The impedance of the strip line is intermediate between that of the junctions and a practical wave guide or coaxial line in the 0.1 to 1 kMHz range. This leads to the possibility of using this geometry as a "transformer", which should markedly improve the possibility of using Josephson junctions as either a generator or detector in this frequency range.

H. The "Normal" Josephson Junction

A crucial point which has not so far been considered is how a device which we will show (page 60) can generate an AC Josephson current of 80 na can avoid having a zero voltage Josephson current of approximately the same size. This is a particularly pertinent question as the coefficient J_1 arises from the same quantum mechanical arguments and, in fact, is the same coefficient; $j = j_1 \sin\delta$ in each case. In the appendix we put forth an argument to explain this apparent discrepancy. The argument is based on the premise that the phase across the Josephson barrier (of resistance R) coupling superconductors (with mean energy gap Δ) is stabilized by the coupling energy $(h/2e)(\pi\Delta/2R)$. If this energy is insufficient to stabilize the phases the relative phase, δ, becomes dependent upon the instantaneous voltage developed across the barrier by thermal noise or other incoherent voltage sources. As a result the Josephson current fluctuates within a band width of $(2e/\hbar)V_{noise}$, and averages to zero. Such junctions show a resistance typical of the Giaever single-particle tunneling and are termed "normal".

For the apparatus we have been considering here the predominant source of noise is the $10^7\,\Omega$ input impedance (Z) of the

amplifier. This noise source is transformed by a turns ratio (η) of 50, filtered (3 dB point about 6 kHz), and applied directly across the comparatively small impedance (R) of the sample. The noise power delivered to the interferometer from the room temperature circuit is then

$$\overline{RI^2_{noise}} = \frac{R\,\overline{V^2_{noise}}}{(R + Z/\eta^2)^2} \approx \frac{4kTR\Delta f}{(Z/\eta^2)} \approx 2R \times 10^{-20}\ \frac{\text{Joules}}{\text{sec}}\ .$$

Comparing this to the coupling energy, $(h/2e)(\pi\Delta/2R)$, the requirement for phase stability is

$$R < \left(\frac{h}{2e}\,\frac{\pi\Delta}{2}\,\frac{\eta^2}{4kTZ\Delta f}\right)^{1/2} \sim (2\times10^{-15}\cdot 1.5\times10^{-3}\cdot 0.5\times10^{20})^{1/2}$$

$$\sim 12\ \Omega \qquad (39$$

which is just the order of junction resistance observed for our samples. The noise voltage corresponding to this power is $V_{rms} \sim 1.4\ R \times 10^{-10}$ volts, which gives a frequency band width $2\delta(hV/2e) \sim 2$ MHz.

If a DC voltage is applied to such a "normal" barrier it will of course have superimposed upon it the same noise voltage that was present before. Now, however, the noise only increases the line width of the otherwise "monochromatic" AC Josephson current by an amount $\frac{2e}{\hbar} V_{noise}$ (peak to peak). In the presence of a "filter", such as the strip transmission line connecting our junctions, only voltage at the frequencies resonantly enhanced by

the strip line are impressed on the junctions by the strip line. When the AC Josephson current has a substantial component at this frequency the demodulation predicted in Equation 25 occurs and an excess DC current is observed. The frequency dependence of this current at the resonances of the strip line is compared with the dependence predicted from the strip line resonance (Equation 37) in Figure 15.

V. EXPERIMENTAL RESULTS AND DISCUSSION

A. Penetration Depths

The depth of penetration of magnetic fields into the superconductors forming the arms of the interferometer significantly affects the behavior of the device. The spacing (in magnetic field) between interference maxima is decreased by the ratio $T/(T + \lambda_1 + \lambda_2)$ where T is the separation of the superconductors. Similarly, the velocity of propagation in the transmission line (and hence its resonant frequencies) is decreased by the square root of this ratio.

As the properties of tin films are relatively well known, the penetration into the tin was calculated from BCS theory (3). The tin films connecting the Josephson junctions actually consisted of three layers each 1300 Å thick, hence, 1300 Å was used for the mean free scattering length. With a coherence length, $\xi_o \sim 2600$ Å this gave a value for λ (0) of 770 Å. For a thin film it is appropriate to use, in place of the penetration depth, λ eff = $\lambda \tanh d/2\lambda$ to properly satisfy the boundary conditions for a film of thickness d with about the same field on each side. With this correction λ eff ranges from 760 Å to 1300 Å for the temperatures used in the experiment. It was possible to obtain the total thickness of the flux sheet at the junctions (where the tin film was 1300 Å thick) from a diffraction pattern obtained with the r.f. interferometer at 1.4°K. After subtracting the calculated penetration into the tin film at that temperature (535 Å) the penetration depth in the niobium was found to be 780 Å. These values for the penetration depths are in relatively good agreement with other determinations and are used throughout the ensuing discussion.

B. DC Interferometer

A de Broglie wave interferometer with $\ell = 0.8$ meters was constructed as described in Section II. B. This interferometer had a zero voltage tunneling current consisting of 12 na of variable current superimposed on a 65 na, flux independent, background. This type of background current is characteristic of Josephson junctions containing superconducting filaments coupling the two superconductors through the barrier. Thus, in spite of the high normal state resistance (60 ohms), the superconducting phase was relatively tightly coupled across the barrier. From the zero voltage interference pattern (Figure 10) a value of $\varphi_I = 2.56 \times 10^{-15}$ webers $= 1.24\ \varphi_o$ was obtained, in reasonable agreement with the accepted value of 2.07×10^{-15} webers if one considers the difficulty of determining the effective area linked by flux in such a convoluted strip line. This value of flux was converted from the measured field values using estimates of the dielectric thickness obtained by capacity techniques, and penetration depths as discussed above. Some 500 interference peaks were observed, apparently enveloped by a diffraction pattern with a basic period of about 1000 peaks, consistent with the dimensions of the junctions. With this interferometer the known range of coherence of de Broglie waves in superconductors was increased by a factor of 25 (actually 250, as reference 14 mentioning a 3 cm interferometer had not yet been published). Further, the validity of the construction and measurement techniques was verified.

C. R. F. Interferometer ("Normal" Junctions)

An interferometer was built with a 1.33 meter superconducting tin film connecting the junctions. It did not show any zero voltage current (< 0.2 na), however, as shown in Figures 5 - 9, below 60 na the I-V characteristic did indicate considerable enhancement of currents above the ordinary Gieaver tunneling current.

Although no zero voltage current was observed, flux dependent structure was noticed in the I-V curve. To enhance this structure recordings of the incremental resistance, dV/dI, vs I_{DC} were obtained using a phase sensitive detector. As predicted by Equation 37, two essentially orthogonal sets of modes were observed. Typical plots of the interferometer current vs voltage are shown in Figures 6 and 9 for m ($= \varphi_I/(\varphi_o/2)$) half integral, even, and odd. These plots are integrals of the incremental resistance versus interferometer current at 1.3°K, recordings of which appear in Figures 5, 7 and 8. Figure 11 is an interference pattern obtained at 2°K using a peak to peak sampling current of 50 na. As a result both the even and odd resonances are excited (n = -1, 0, +1) and appear as interlaced interference patterns of different amplitudes. In Figure 11, m = 0 to +400; an essentially identical plot was obtained for m = 0 to -400. Interference patterns were also obtained with several sampling currents and with various DC bias currents through the sample. With a sufficiently small sampling current, it was observed that a separate interference pattern could be obtained for each mode. These patterns were interlaced, corresponding to maxima occurring at even or odd m, depending on the bias current (i.e., on β), in complete agreement

with Equation 37. The basic interference period ($\Delta m = 2$) was about .60 mG. Combining this with the capacitively determined dielectric thickness (.68 μ), the temperature dependent penetration depths as discussed in Part A of this section, and the junction spacing of 2.58 cm gives $\varphi_I = 1.27 \times 10^{-15}$ webers = 0.615 φ_0. The statistical variation of this result is about 2% (based on various measurements of the interference period).

This result for the AC interferometer is fairly close to $\varphi_0/2$, and is almost exactly half the value (1.24 φ_0) obtained with the 0.8 meter DC interferometer. It is thus tempting to explain the data in terms of "multiple pairs" i.e., $e^* = 4e$. Such a concept was suggested by Little and Parks (15) to explain some of their data on the periodicity of the transition temperature of superconducting tubes with magnetic field. There is, however, no theoretical justification for such an explanation. Furthermore, Douglass (16) has shown that in a doubly connected superconductor nonlinearities do not generate any such "harmonics" of the unit quantum. He has also suggested a possible alternate explanation for the Little and Parks data.

In our case we have $\varphi_I \sim .6\ \varphi_0$. If we reject the hypothesis of "multiple pairing" we must find an alternate explanation for the discrepancy. Systematic errors in measurement of the junction separation, calibration of the solenoid in the superconducting shield and instrumental errors perhaps total 10%, leaving a residual discrepancy of about 30%. Obviously the experimental agreement is not very good. However, effective area determinations on these large samples are relatively difficult, particularly as non-destructive methods must be used. Our result corresponds to an area about 60% larger than the experimentally determined area, or an excess area

(such as a "bubble" in the Formvar film) equivalent to 25 μ by 1 mm. Such a defect would be difficult to detect.

The velocity of propagation (and hence the resonant frequency of the strip line) is less sensitive than the interference period to the presence of localized non uniformities in the dielectric, consequently we would expect closer agreement between the calculated and experimental frequencies.

The resonant frequencies of the strip transmission line are obtained immediately by combining Equations 26 and 38. Thus,

$$\frac{\omega_r}{2\pi} = \left(\frac{\beta_r}{2\pi}\right)(v_p) = \left(\frac{g(n)}{2\ell}\right)\left(\frac{c}{\sqrt{\epsilon_r}}\sqrt{\frac{T}{D}}\right) = A\ \frac{D(0)}{D(t)}\ g(n) \qquad (40$$

where A = 60.9 MHz and D(t) represents the value of $T + \lambda_1 + \lambda_2$ at the reduced temperature t. We have used the tabulated value (AIP handbook) $\epsilon_r = 2.8$ for the Formvar dielectric above 10^7 Hz (assumed not to depend on temperature below 26°C). The experimental data are compared with this prediction by computing a value for A at each data point. The Josephson condition, V = hf/2e, is used to convert the DC voltage corresponding to each maxima of excess current on the integrated curves (Figure 9) to a frequency. Each of these frequencies is corrected for temperature and resonance number using Equation 40, giving an experimental value of A_x to compare with the predicted value 60.9 MHz. Values of A_x calculated in this way are displayed vs n and t in the table. The unweighted average of all values of A_x in the table is 63.5 MHz ± 10 MHz, in good agreement with the value independently calculated from the strip line parameters. There appears to be an obvious

TABLE I

Experimental Values of "A" at Different Temperatures as a Function of the Resonance Number, n

T(°K)	Resonance Number 1 [11	2 12	3 13	4 14	5 15	6 16	7 17	8 18	9 19	10 20]	Weighted Average	Deviation from $\overline{A_x}$
3.66	90.2	87.6	71.7	77.7	73.0						77.72	+14.46
3.635	62.9	78.5	78.4	74.1	74.9						75.17	+11.91
3.49	75.0	72.2	65.3	65.5	67.5						67.86	+ 4.60
3.36	74.9	80.4	66.3	74.3	66.1	70.6					71.17	+ 7.91
3.06	51.3	49.2	42.8	43.8	46.5	42.0					45.00	-18.26
1.975	74.8	77.0	60.4	66.1	60.6	63.2	59.8	58.8	59.7	57.2	60.38	- 2.94
	[-	57.8	-	57.2	-	55.8	-	57.1	-	55.4]		
1.975	68.2	62.9	55.3	55.5	53.6	53.4	51.8	52.7	52.9	52.9	54.35	- 8.91
	[53.2	51.9	-	-	-	-	-	-	-	-]		
1.4	-	59.5	51.2	52.1	52.9	54.0	54.0	54.0	53.6	55.8	54.45	- 8.82
	[54.0	55.8	54.4	55.5	54.9	55.9	55.0	-	54.8	-]		
											63.26	± 9.91
											57.0	± 8.9

Mean of Eight Runs --- $\overline{A_x}$ =

Fundamental Resonance Frequency $\overline{f_o} = .9\overline{A_x}$ =

decrease in A_x with increasing n or t. However, the location of the n = 1 and 2 current peaks was uncertain by at least 20% and 10% respectively, due to the relatively large slope of the excess current curve near zero applied voltage. This slope would tend to make the peak appear at an excessively high voltage. In averaging the data these points were weighted 1/3 and 2/3 respectively as no reasonable criterion was available to aid in more accurately locating these peaks. In view of this uncertainty the dependence of A_x on n is much less noticeable. The residual dependence is probably due to the difficulty in determining the constant of integration, R_o, when reconstructing the I-V curve from the dV/dI = R vs I curves. In general, the DC signal out of the phase detector was noted relative to the signal with zero drive current. However, there was some cross-talk in the circuit so that even with R = 0 the phase detector output was somewhat dependent on the drive current. A best estimate, based on a single measurement of the cross-talk, was used throughout the data analysis. However, it is likely that the actual cross-talk changed from time to time, depending on the location of leads and equipment.

The most obvious scatter in the data is that between different runs, i.e., at different temperatures. This is undoubtedly due to uncertainties in setting the 2 na sampling current used in obtaining the dV/dI curves. This was reset for each run at a given temperature and could only be set to about $\pm$ 10% accuracy. The temperature correction D(0)/D(t) was in the wrong direction to improve the correlation between the data taken above 3.4°K and below 3.4°K (where the correction was negligible). However, this correction was always less than 5%. Using n instead of g(n) to compute values of A_x at a given temperature, such as 1.4°K, gave

about 4 times the standard deviation as well as giving an obvious systematic increase of A_x with n. Thus, although the individual data points show considerable scatter, this scatter is largely attributable to experimental uncertainties. The average of all the experimental data agrees within 5% with the value predicted from Equation 40 and (as we shall see) with the frequency effective in stimulating the strip line externally.

Let us now consider the resonant denominator of Equation 37. This denominator determines the frequency dependence of the excess DC current at resonance, (except for variations of $\beta\ell$ from $n\pi$). Each term in the denominator has previously been discussed with the exception of R and $\tan\delta$. The term $2Z_o/R$ is not frequency dependent; however, the low voltage junction resistance is temperature dependent, $R \sim 46\ T^{-1.5}$. The tabulated value of the loss tangent for Formvar at 300^oK and 10^7 Hz is 0.0165, at 3×10^9 Hz is 0.0113. Experimentally the leakage conductance at 1000 Hz has been found to decrease by a factor of 8 between 300^oK and 77^oK. Thus, a reasonable low temperature value for $\tan\delta$ between 10^8 and 10^9 Hz is 0.0015. Combining this with the parameters of the strip line we have immediately

$$\alpha_d \ell = \frac{Z_o\, w\ell\, \omega\epsilon \tan\delta}{2\,T} = 0.012\ \frac{\omega}{\omega_o}\ Z_o\ .$$

The denominator of Equation 33 may now be written

$$\text{Den} = Z_o\left[.043\ T^{1.5} + .012\,\frac{\omega}{\omega_o}\left(1+\left(.2\,\frac{\omega}{\omega_o}\right)^2\right)\right] \qquad (41$$

where $T^{1.5}$ indicates the observed temperature dependence of the junction resistance. In Figure 15 the reciprocal of (Den) is plotted against frequency for several temperatures and is compared with the excess DC current observed at those temperatures. The curves calculated from Equation 41 were adjusted vertically to fit the $T = 1.90^{o}K$ data. The $1.4^{o}K$ data seem to be shifted to the right by about a factor of two. No explanation of this effect is available.

An interesting sidelight of the analysis of self generated effects is the possibility of calculating the magnitude of the AC Josephson current from our essentially DC measurements. If I_{DC}/I_1 is much less than unity we can expand the Bessel function in Equation 37, i.e., $J_1(x) \sim x/2$. Approximating the cosine and sine terms by unity at resonance, and taking a sufficiently low frequency that the dielectric losses are negligible we have

$$I_1 = (I_{DC}^{\text{resonant}} \frac{\hbar}{2e} \frac{2}{c Z_o R})^{1/2} . \qquad (42$$

At $1.4^{o}K$, the excess direct current is 10 na. Inserting values for the flux quantum and the various circuit parameters gives

$$I = \left(\frac{10^{-8} \cdot 2 \times 10^{-15} \cdot 2}{4 \times 10^{-9} \cdot 0.15 \cdot 15} \right)^{1/2} = 80 \text{ na} .$$

Thus, the AC Josephson current flowing through the junctions is about 80 na. Half of this flows through each of the 27 Ω junctions producing an AC voltage of about 1 μv to drive the strip transmission line. Because of the impedance mismatch about 1% of this voltage

appears in the strip line. It is resonantly enhanced and fed back to the junctions to produce the 10 na of excess current observed. The 80 na of AC current is about 1000 times smaller than the value predicted by Josephson, i.e., $\pi\Delta/2R \sim 100\ \mu a$ (where Δ is the half energy gap, about 1 mv). However, 80 na multiplied by the inductance of the strip line, $\mu_o \ell\ t/w \sim 10^{-9}$h, produces a flux of $\sim 10^{-16}$ webers = $\varphi_o/20$, sufficient to shift the interferometer away from the resonance condition. The AC current will thus be self limiting at about this level.

D. Response to External RF Stimulation

The above discussion has been confined to self generated effects predicted by Equation 25. The interferometer will also respond with a time independent current proportional to $J_N(v/V)$ whenever it is stimulated by radiation at frequencies, ω, which are submultiples of the Josephson frequency $\Omega = 2eV/\hbar$.

As a final test of the validity of the general analysis based on the AC Josephson effect, the influence of externally applied RF was observed. The de Broglie wave interferometer was adjusted to a voltage corresponding to the second resonance peak ($n = 2$, $\lambda \sim L$) and the magnetic field was adjusted to produce minimum current enhancement. Under these conditions the frequency of an external RF generator was swept over the band from 65 MHz to 1 MHz (higher frequencies were not available). Coupling was accomplished through a 70 db attenuator in the Dewar cap leading to a twisted pair ending in a small multiturn coil inside the solenoid. Current enhancement was observed only between 45 and 57 MHz. Maximum effect occurred at 55 MHz in agreement with the resonant frequency of the strip line calculated in from Equation 30. At this

frequency the input level was varied from 0 to 100 mv and the incremental resistance (dV/dI) was observed. Under these conditions Equation 25 predicts a dependence on the applied r. f. voltage like $J_2(v/V)$. In Figure 16 we plot this function. The experimental values of dV/dI were fitted near the top of the first maximum. The general agreement is comparable to that obtained by others on single junctions in microwave cavities.

VI. CONCLUSIONS

Superconducting links 0.8 and 1.33 meters in length have successfully been used to couple two Josephson junctions, forming de Broglie wave interferometers. Although these quantum interferometers are 40 times larger than any previously reported, there is no indication of a breakdown of quantization. Quantum phase coherence of the de Broglie waves has thus been demonstrated in these truly macroscopic systems. Although the interferometer length exceeds a meter and the number of electrons involved is of order 10^{20}, recourse to classical physics through the correspondence principle is not possible. The states of the system are only calculable directly in terms of the quantum of action, $\hbar$.

The interactions between the de Broglie wave interferometer, the electrodynamics of the superconducting strip line structure, and the AC Josephson effect have been analyzed in detail and experimental observations have confirmed the basic understanding of these phenomena. A superconducting cavity has thus been utilized here -- in analogy with the maser -- to provide coherence between junctions decoupled by thermal noise, resulting in quantum oscillation at the cavity frequency.

Evidence for oscillations at all harmonics of the fundamental frequency of the strip line up to the 27^{th} (about 1.5 kMHz) was obtained. This suggests the possibility of utilizing strip lines as "transformers" to enhance the generation or detection of radiation by Josephson junctions.

REFERENCES

1. F. London, Proc. Roy. Soc. A 152, 24 (1935).
2. F. London, Phys. Rev. 74, 562 (1948).
3. J. Bardeen, L. N. Cooper, and J. R. Schrieffer, Phys. Rev. 108, 1175 (1957).
4. R. Doll and M. Nabauer, Phys. Rev. Letters, 7, 51 (1961).
5. B. S. Deaver and W. M. Fairbank, Phys. Rev. Letters 7, 43 (1961).
6. I. Giaever, Phys. Rev. Letters 5, 464 (1960).
7. B. D. Josephson, Physics Letters 1, 251 (1962); Rev. Mod. Phys. 36, 216 (1964).
8. J. M. Rowell, Phys. Rev. Letters 11, 200 (1963).
9. I. K. Yanson, V. M. Svstunov, and I. M. Dmitrenko, E. H. Ekserim. i Teor. Fiz. 48, 976 (1965).
10. M. D. Fiske, Rev. Mod. Phys. 36, 221 (1964).
11. R. C. Jaklevic, J. Lambe, A. H. Silver, and J. E. Mercereau, Phys. Rev. Letters 12, 159 (1964).
12. R. C. Jaklevic, J. Lambe, J. E. Mercereau, and A. H. Silver, Phys. Rev. 140, A1628 (1965).
13. L. P. Gor'kov, Zh. Eksperim. i Teor. Fiz., 36, 1918; 37, 833 (1959); Translation Soviet Phys. JETP, 9 1364; 10, 593 (1960).
14. P. W. Anderson, Lectures on the Many Body Problem, Vol. 2, edited by E. R. Caianiello, (Academic Press, 1964) p. 113.

15. W. A. Little and R. D. Parks, in Proceedings of the Eighth International Conference on Low Temperature Physics, Butterworths, London (1963), p. 129.

16. D. H. Douglass, Jr., Phys. Rev. 132, 513 (1963).

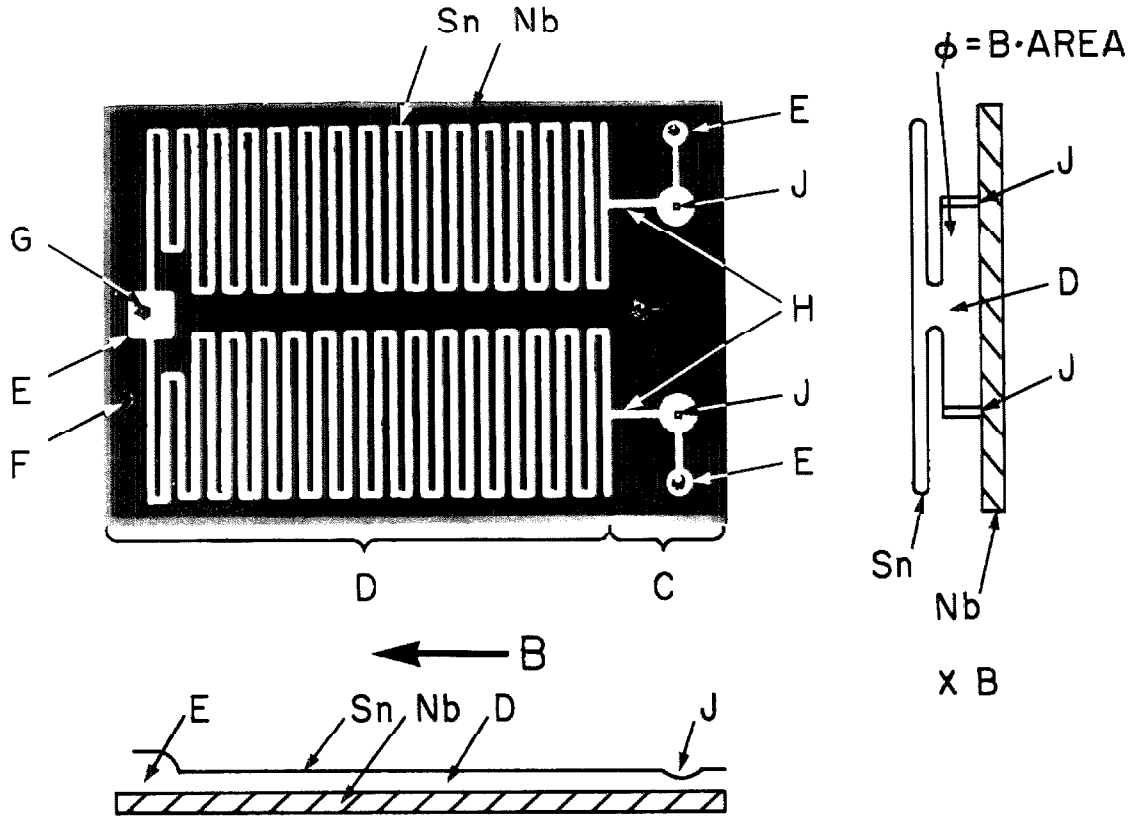

FIGURE 1

1.33 Meter de Broglie Wave Interferometer: the Niobium Sheet is 50 mm by 75 mm, and is Approximately to Scale.

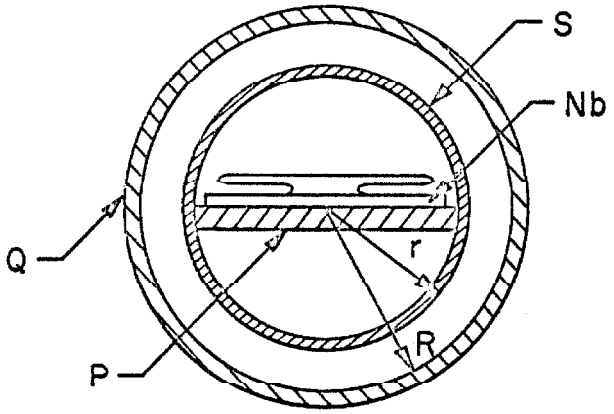

FIGURE 2. Arrangement of Solenoid (S), Superconducting Shield (Q), and Sample (Nb)

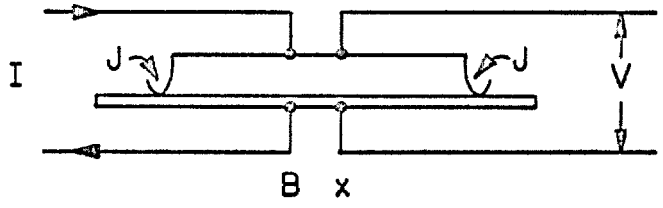

FIGURE 3. Electrical Connections to Interferometer

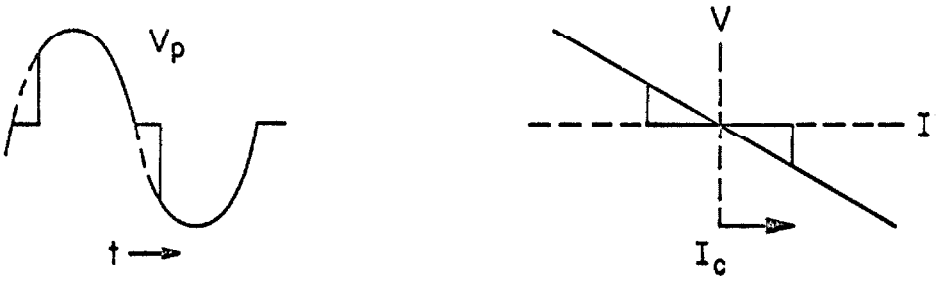

FIGURE 4. V-t and V-I Waveforms for a Josephson Junction

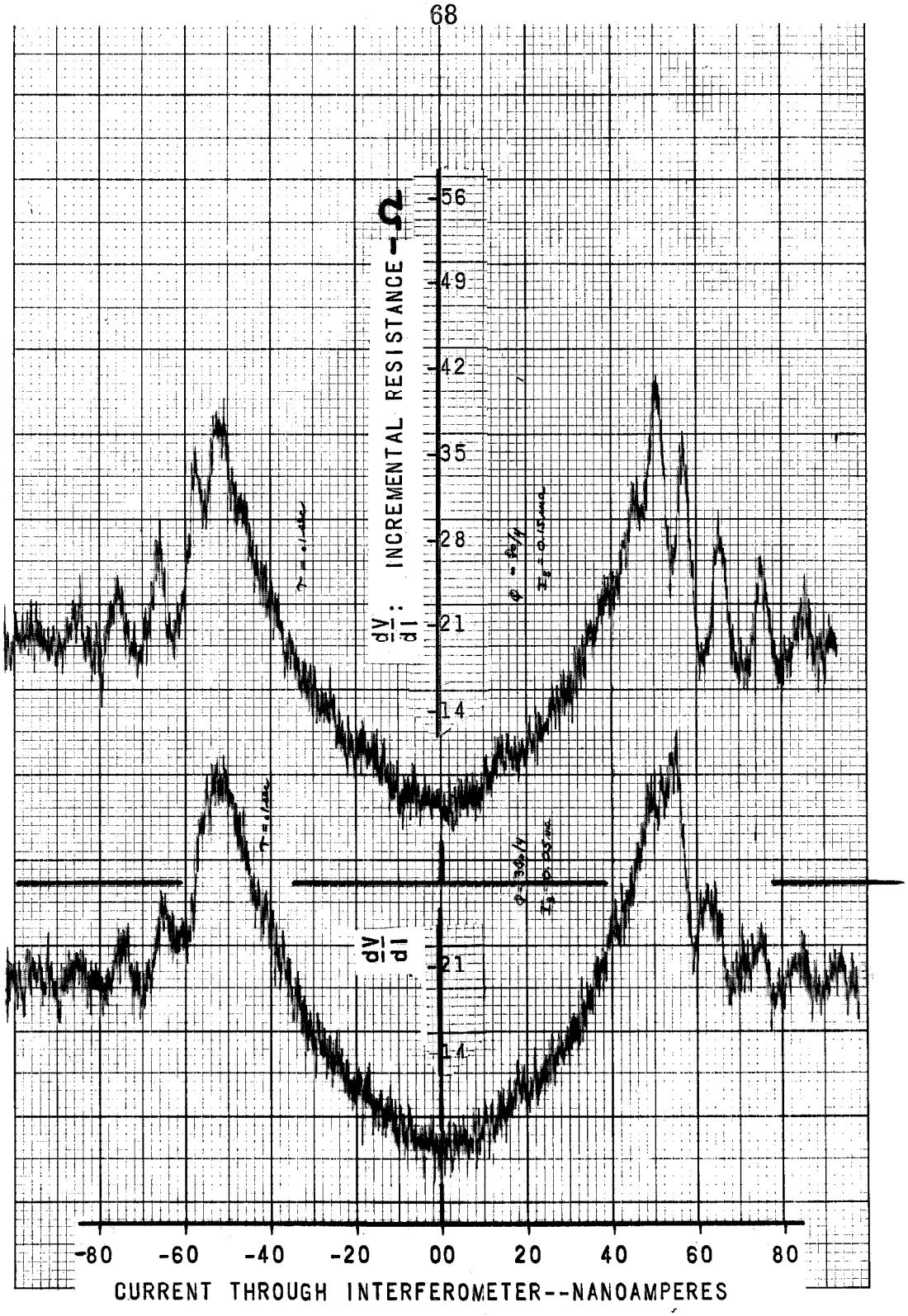

FIGURE 5. dV/dI-I Curve: Magnetic Field Adjusted to Between Modes ($\varphi = 3\varphi_o/4$, $\varphi_o/4$).

Integrated Curve in Figure 6.

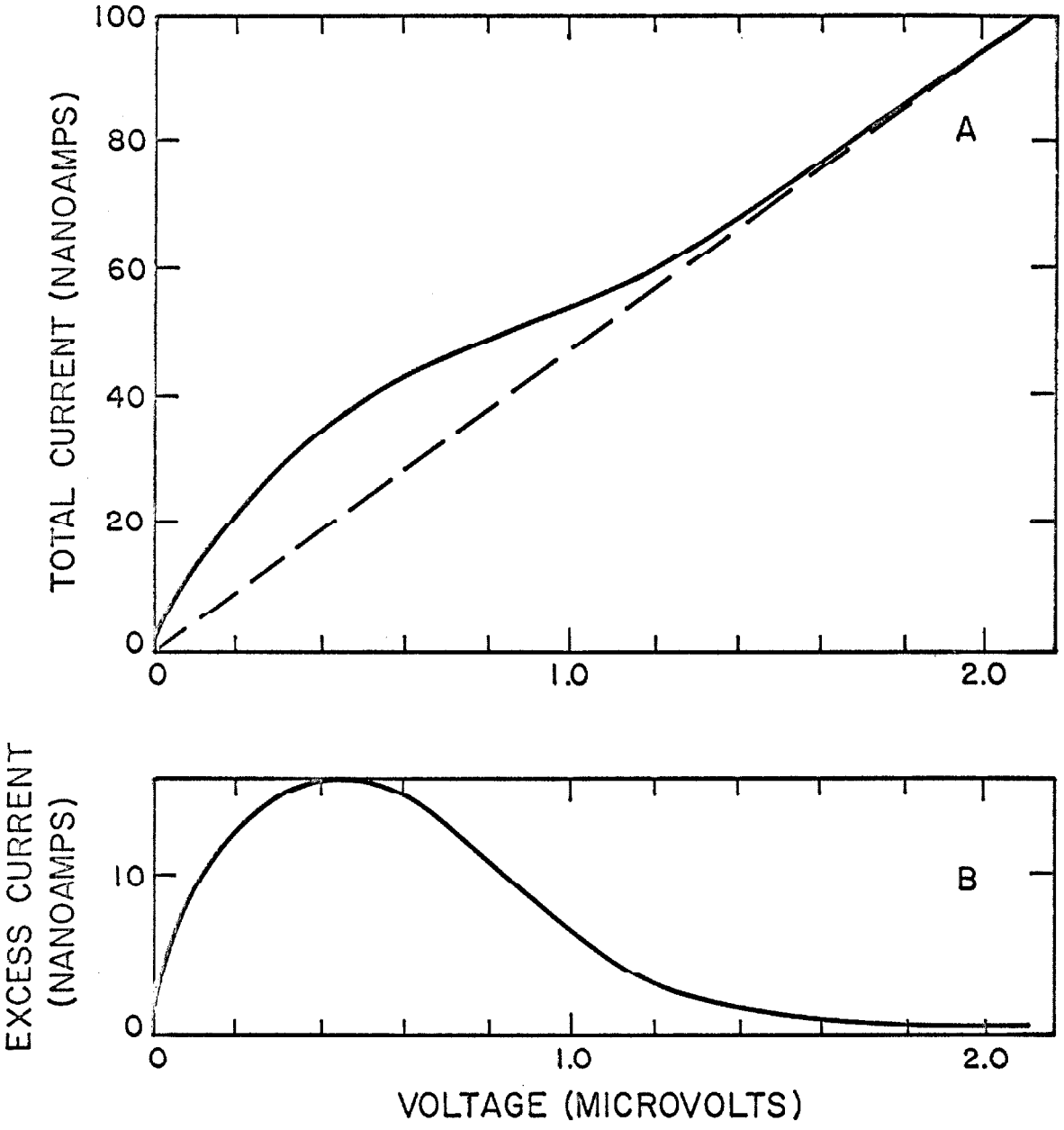

FIGURE 6. A. Integral of Figure 5; I-V Curve of "Normal" Interferometer Operating Between Resonant Modes

B. Excess Current from Curve A

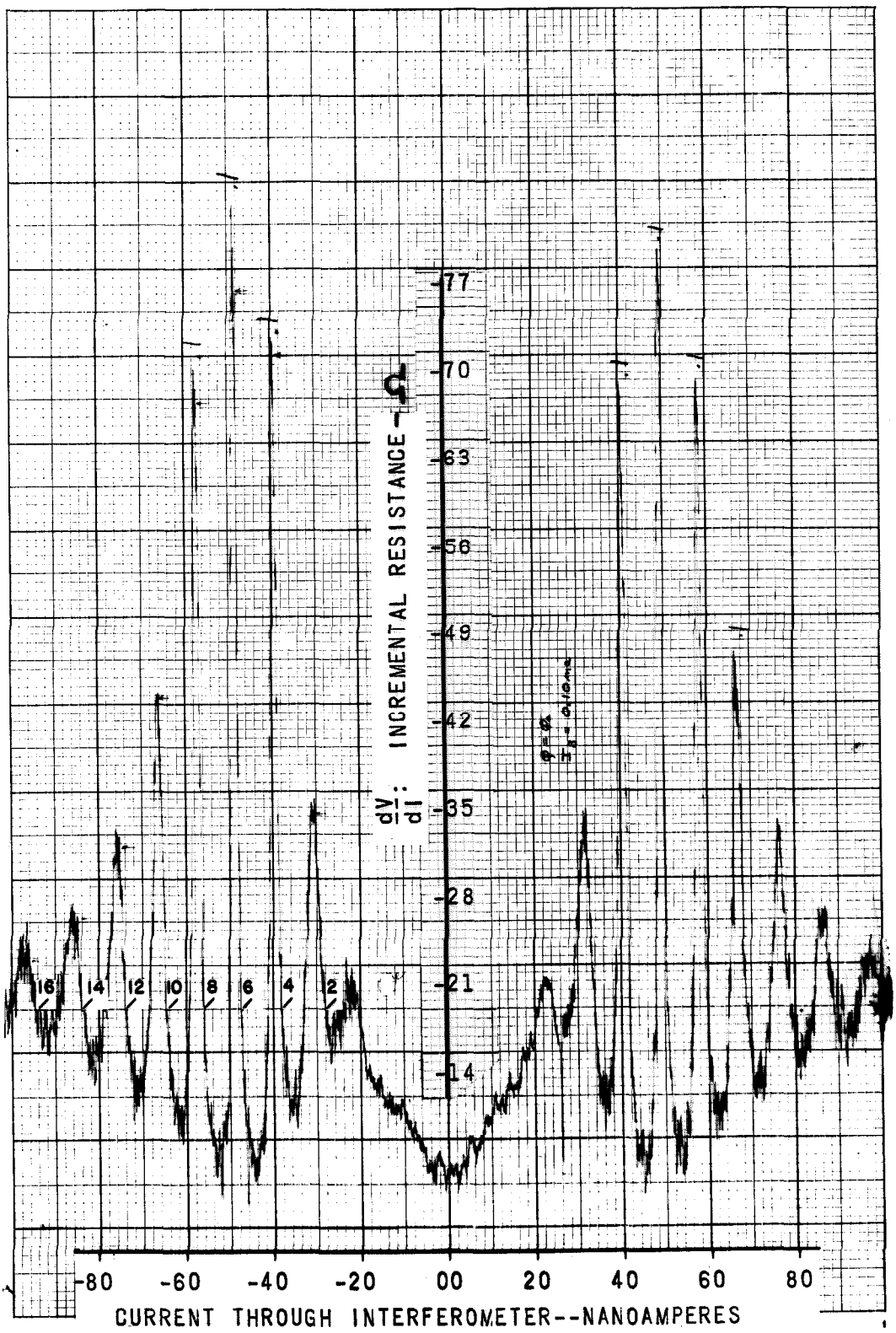

FIGURE 7. dV/dI-I Curve: Magnetic Field Adjusted to Even Modes ($\varphi = \varphi_0$).

Integrated Curve in Figure 9 (solid line).

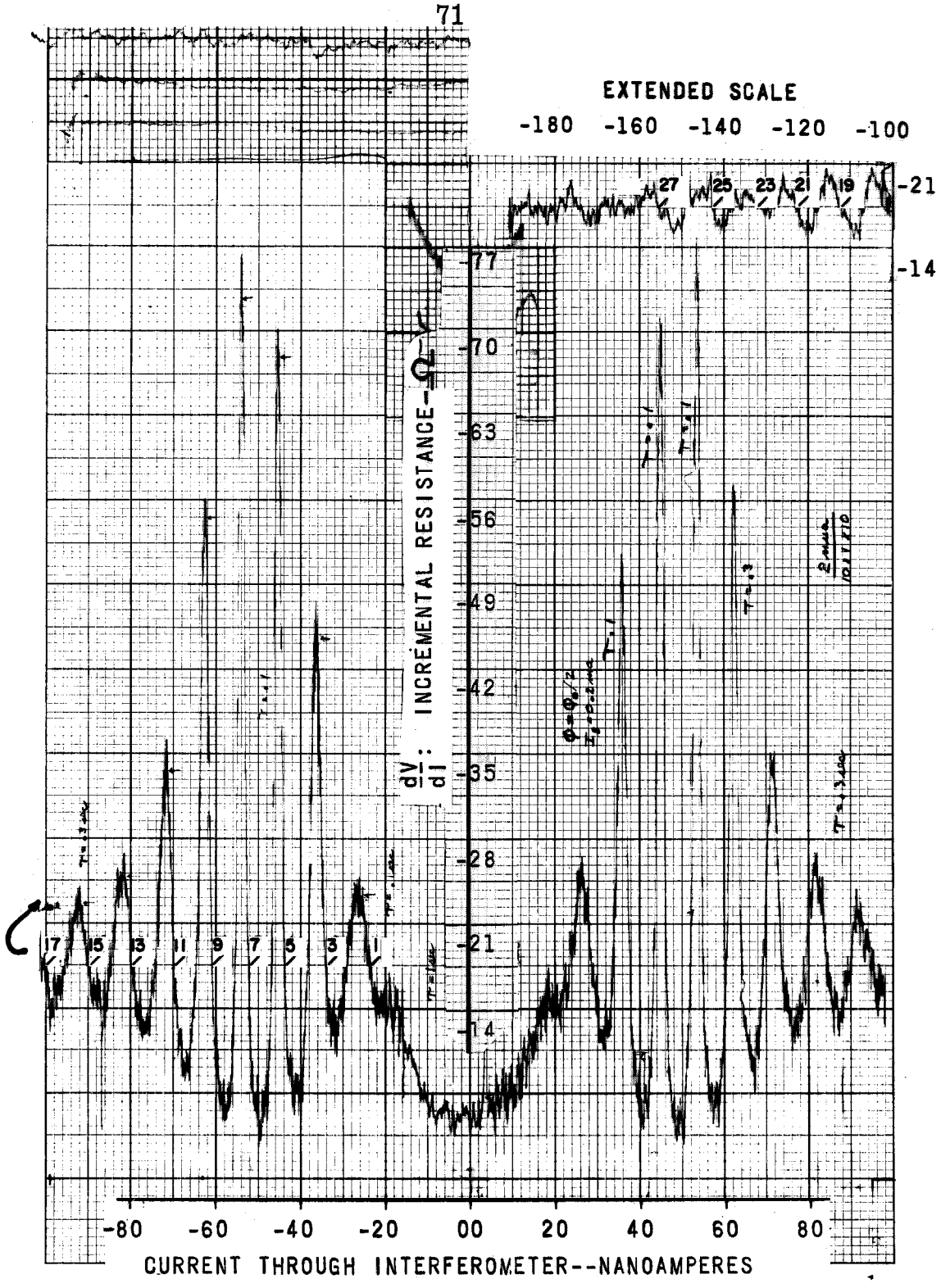

FIGURE 8. dV/dI-I Curve: Magnetic Field Adjusted to Odd Modes ($\varphi = \varphi_0/2$).

Integrated Curve in Figure 9 (broken line).

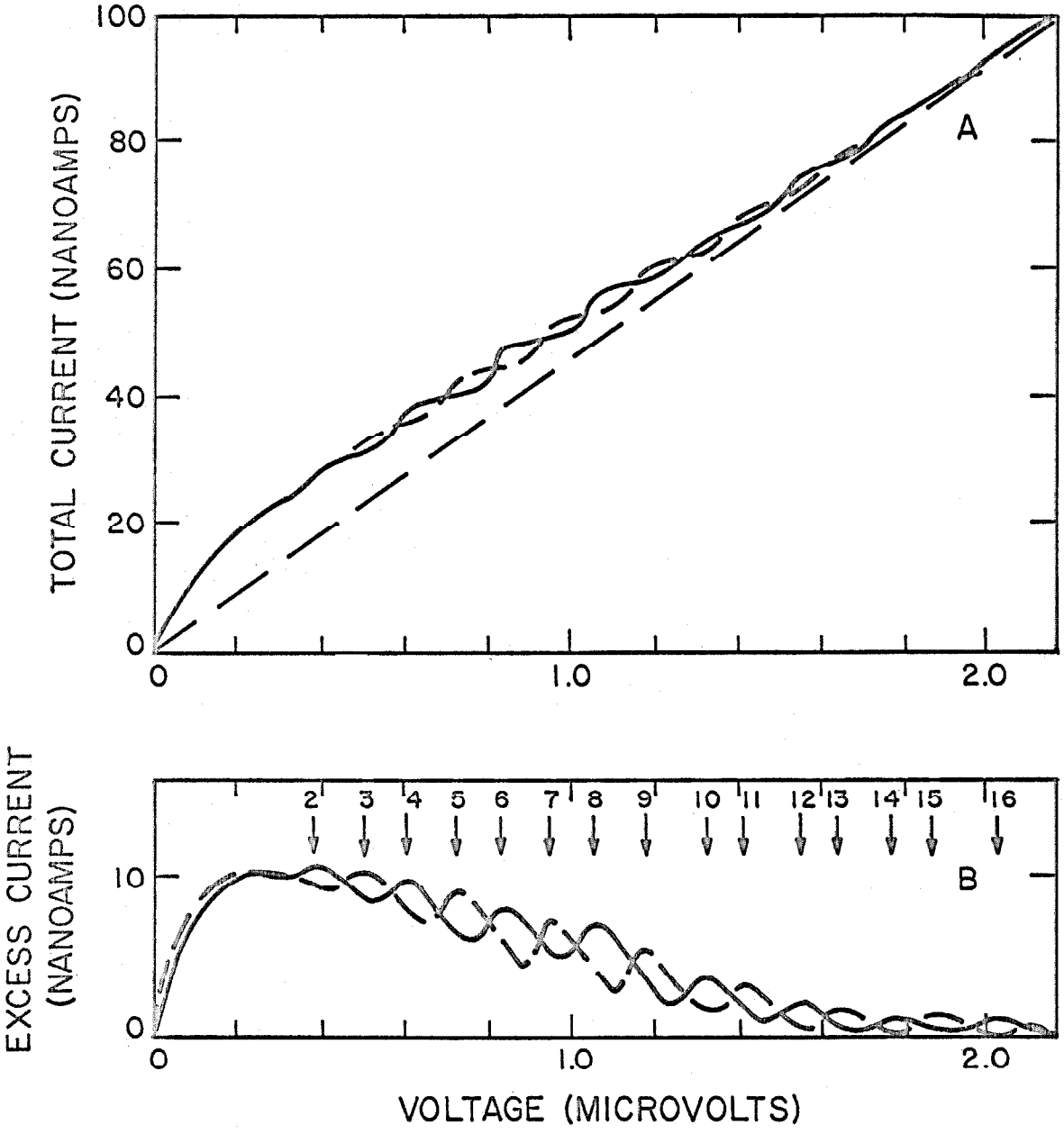

FIGURE 9. A. Integrals of Figure 7 (solid line) and Figure 8 (broken line); I-V Curve of "Normal" Interferometer Illustrating Alternation of "Constant Voltage" Steps

B. Interlaced Excess Current Peaks from Curves A

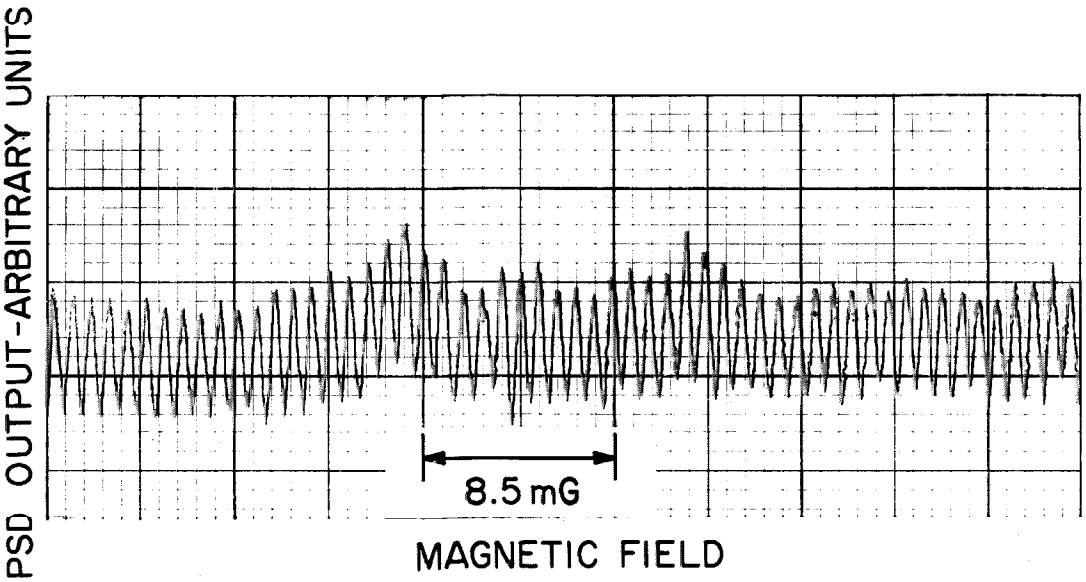

FIGURE 10

Interference Pattern: DC Interferometer

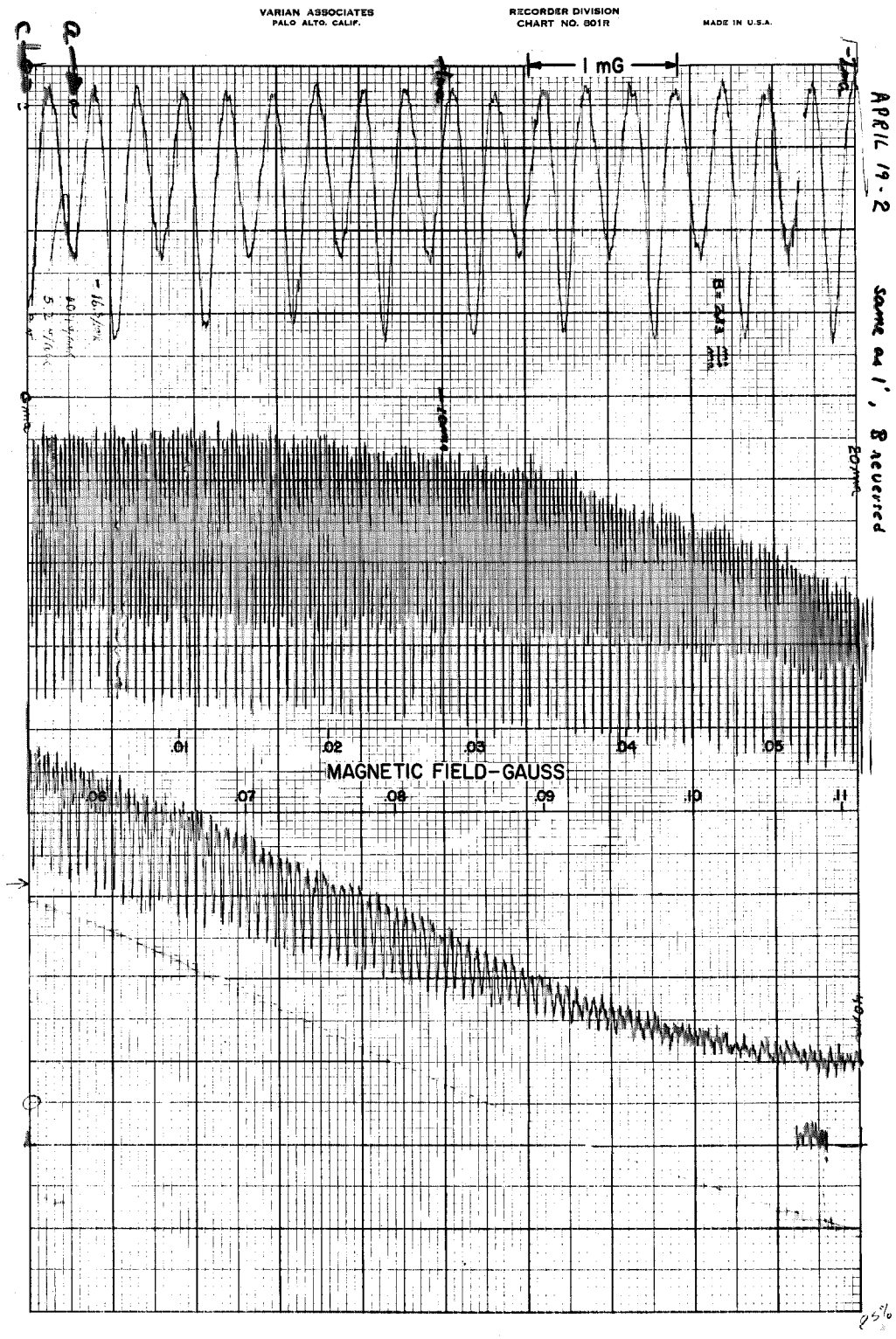

FIGURE 11

Interference Pattern: AC Interferometer

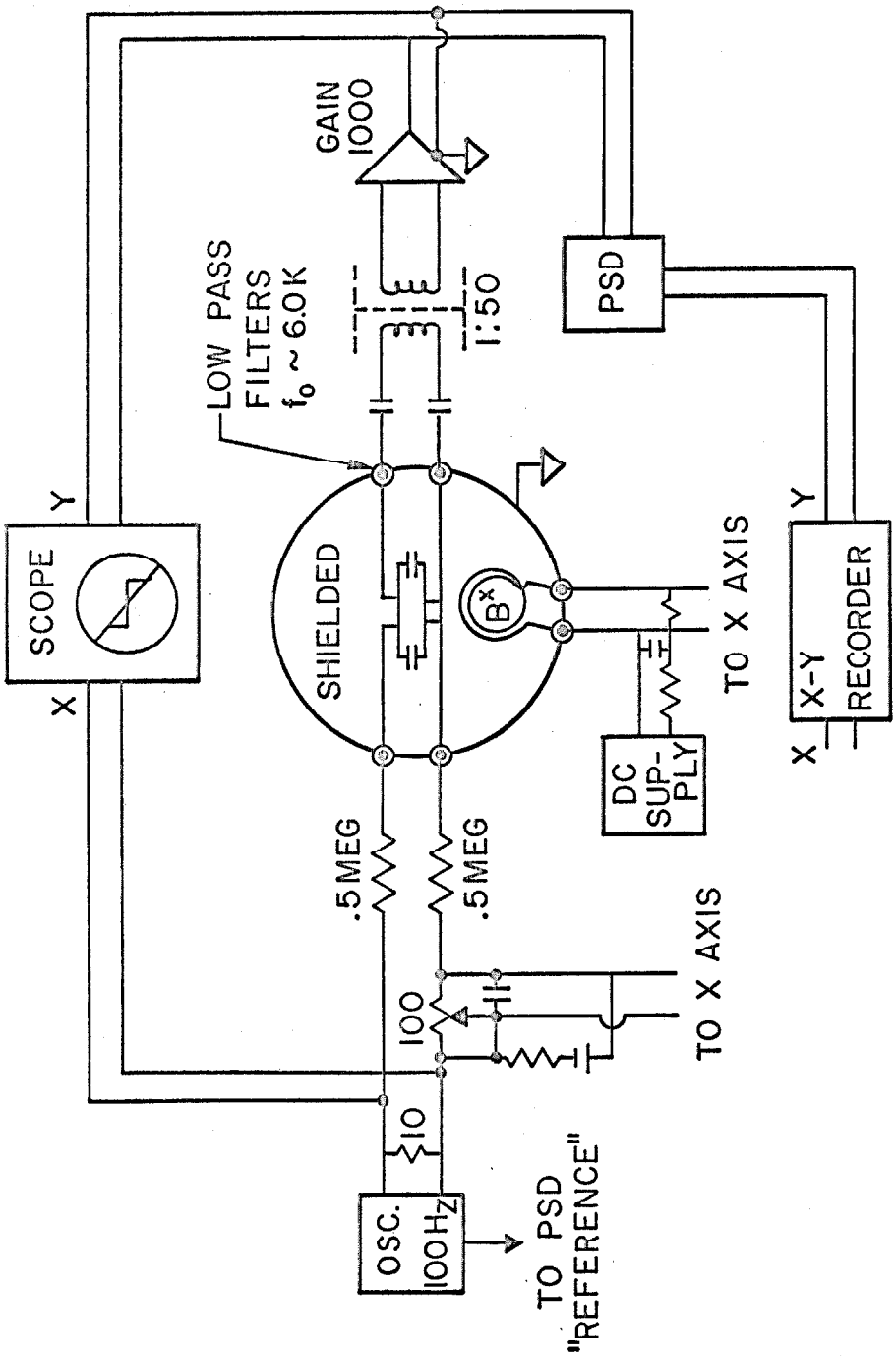

FIGURE 12. Schematic Circuit Diagram: The Shielded Region is at Helium Temperature

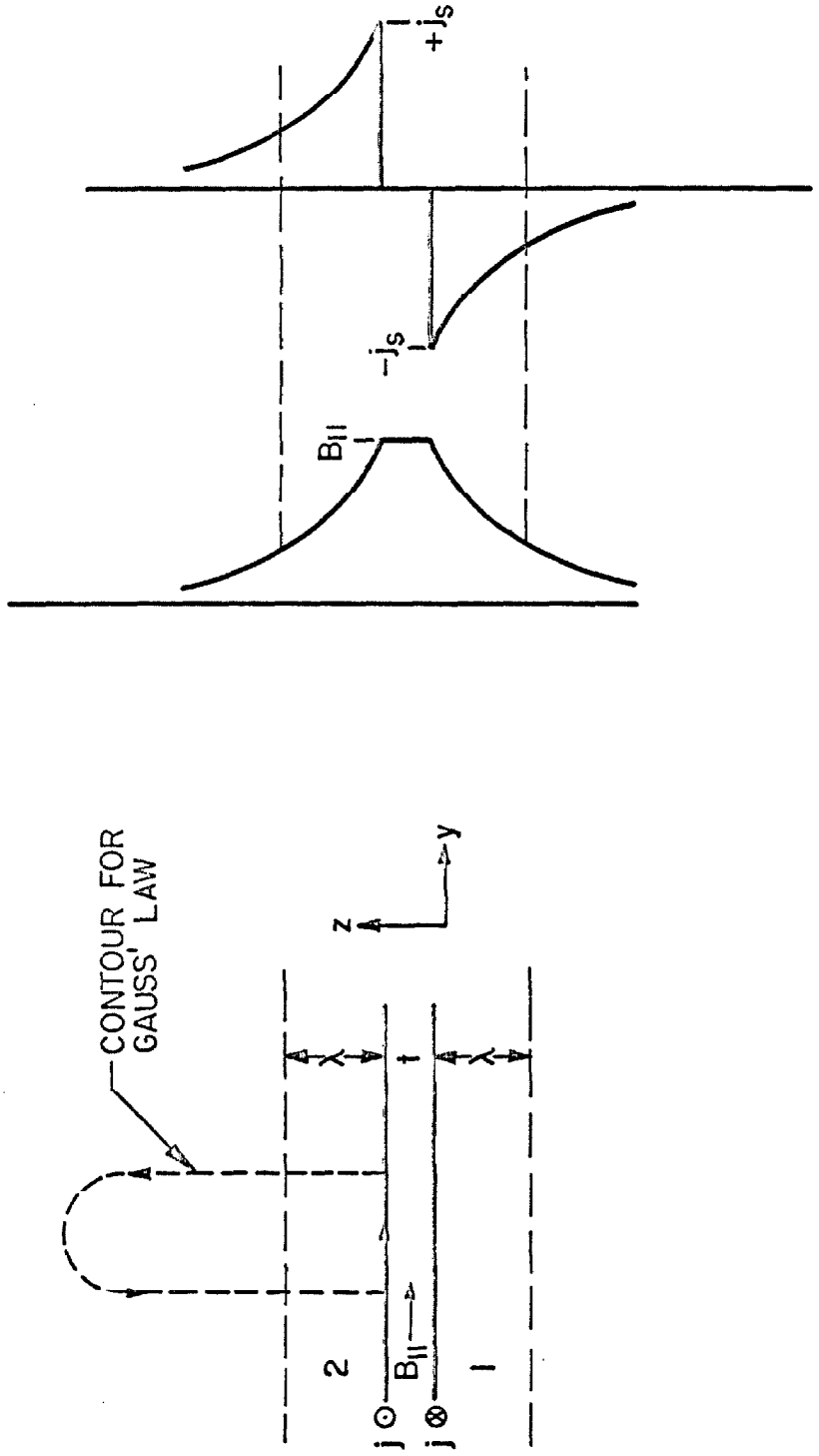

FIGURE 13. Relation of Penetration Depth, Magnetic Field, and Screening Supercurrents at a Junction

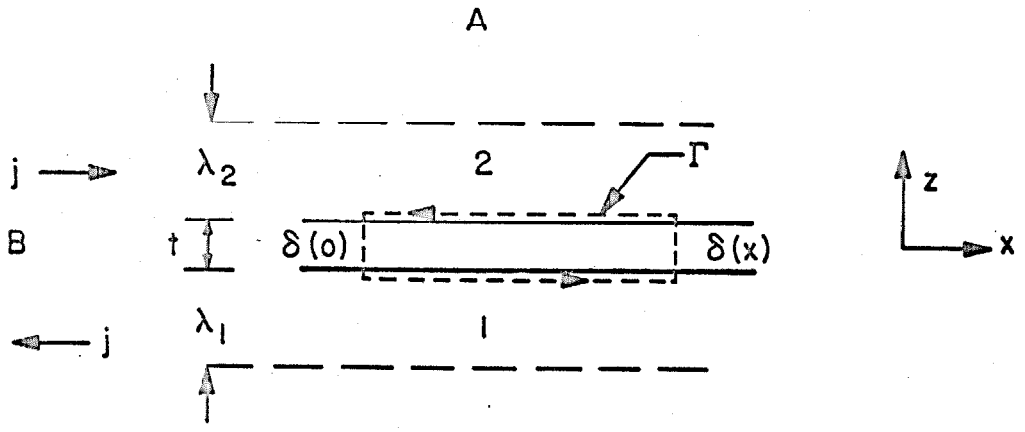

a) Schematic of Josephson Junction Indicating Contour for Computing Phase Difference $\delta(x)$

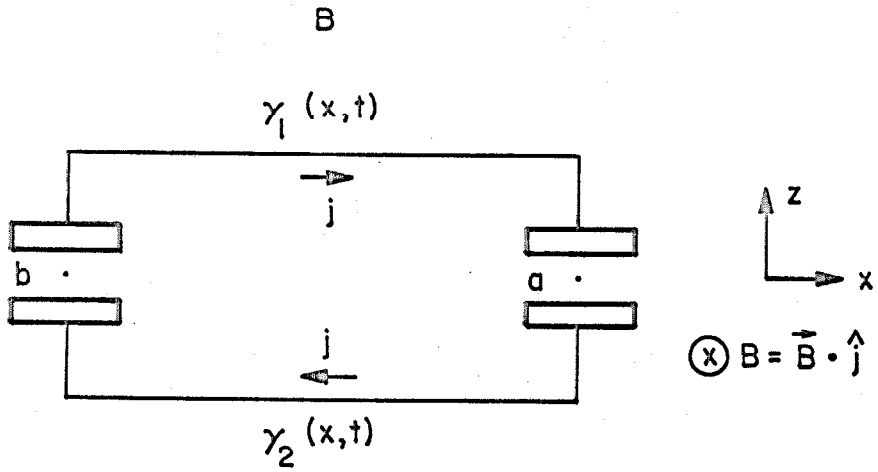

b) Schematic of de Broglie Wave Interferometer

FIGURE 14

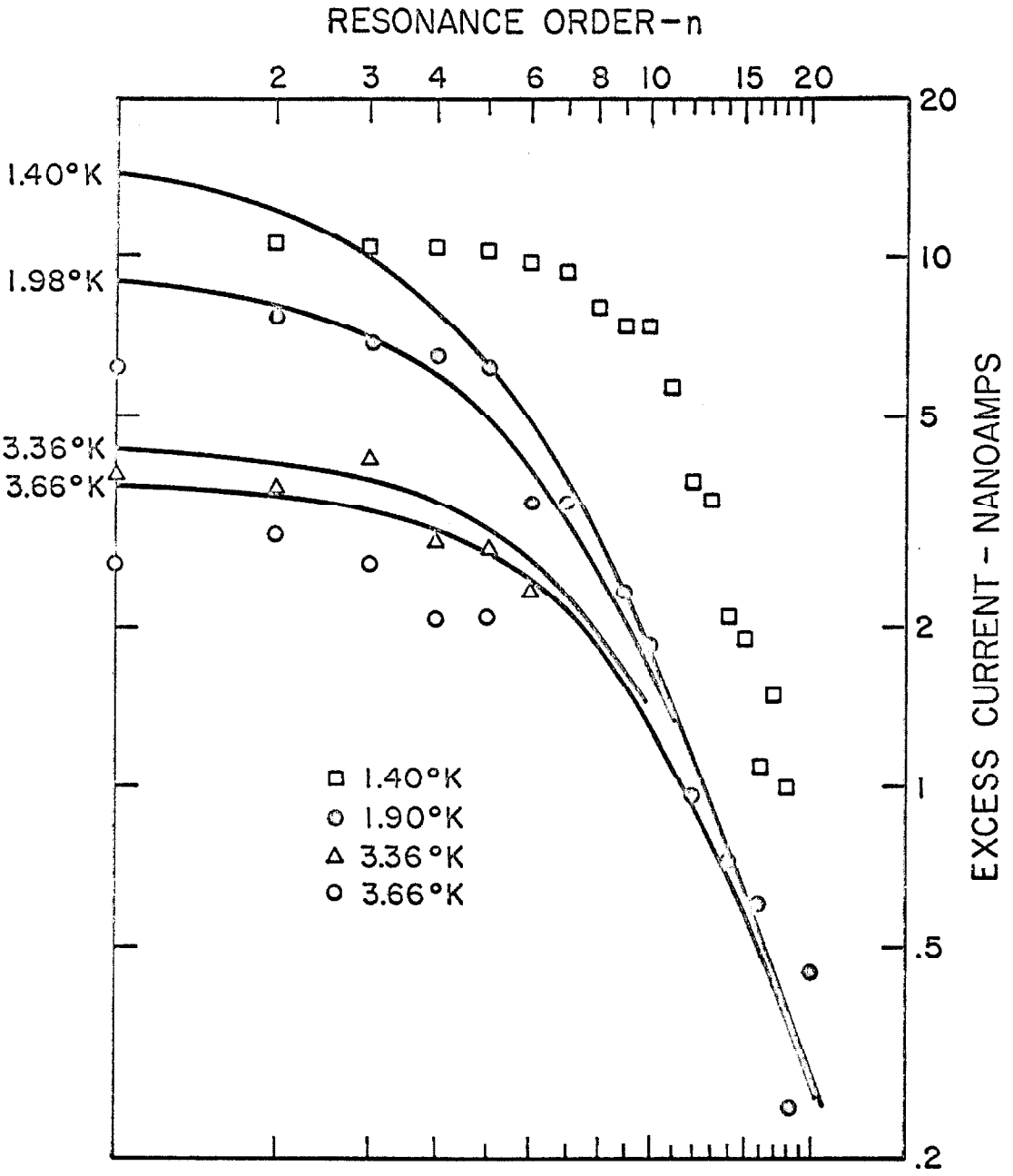

FIGURE 15. Excess Tunneling Current vs Frequency (or Resonance Number-n) at Several Temperatures: The Solid Curves are Calculated from Equation 41

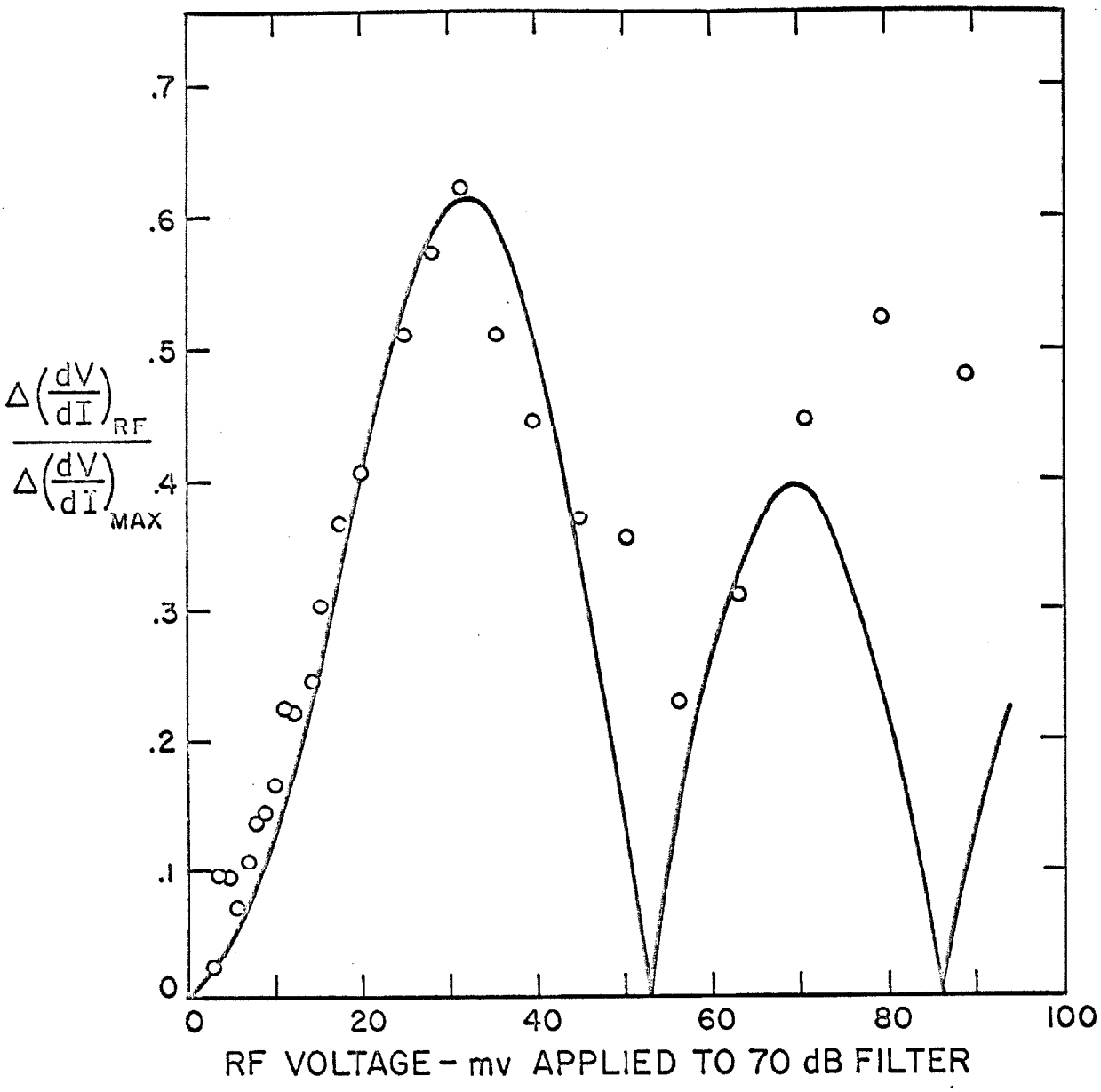

FIGURE 16. Effect of Applied 55 MHz Radiation: The Solid Curve is a Plot of $J_2(x)$ Fitted Between 20 and 30 mv

APPENDIX

"Normal" Josephson Junctions and Quantum Coherence. L. L. Vant-Hull and J. E. Mercereau.

Reproduced From Physical Review Letters Volume 17, Number 12, 19 September 1966, pages 629, 630 and 631.

"NORMAL" JOSEPHSON JUNCTIONS AND QUANTUM COHERENCE

L. L. Vant-Hull and J. E. Mercereau
California Institute of Technology, Pasadena, California,
and Ford Scientific Laboratory, Newport Beach, California
(Received 6 July 1966)

Supercurrent through Josephson barriers[1] has been widely studied with a particular fascination because of the essential quantum nature of the phenomenon. The behavior of this supercurrent is determined by the relative quantum phase across the barrier. If the coupling energy of the Josephson junction is sufficient to stabilize this relative phase against noise, a zero-voltage supercurrent can flow. However, if the coupling energy is too small to provide phase stabilization, the relative phases become incoherent and the supercurrent averages to zero. In this "normal" state of the junction[2] a coherence forced upon the radiated electromagnetic fields can serve to stabilize the behavior of the junction. The purpose of this Letter is to report evidence for such induced coherence in "normal" junctions, and to report the use of a "normal" quantum interferometer to determine phase coherence in a superconducting film 1.33 m long.

Josephson supercurrent density $j = j_0 \sin(\gamma_1 - \gamma_2)$, relating current through a barrier to the quantum phase, can easily be integrated over sufficiently small barriers to yield an expression for total supercurrent (I),

$$I = I_0 \frac{\sin[(e/\hbar)\varphi_J]}{(e/\hbar)\varphi_J} \sin(\Delta\gamma). \qquad (1)$$

In this integration the dependence of phase on vector potential is explicitly exposed in the diffractionlike dependence of current on magnetic flux φ_J within the junction. However, the current also depends sinusoidally on the residual phase difference ($\Delta\gamma$) across the barrier. Thus, the existence of a net supercurrent depends on the stability of $\Delta\gamma$. A stable $\Delta\gamma$ adjusts to be as small as possible, consistent with a given current source, leading to the observed[3] diffractive behavior of maximum supercurrent with flux.

If the coupling energy, $(\hbar/2e)(\pi\Delta/2R)$ is small —a high-resistance (R) barrier, for example —the noise in the circuit may cause a decoupling of phases. In the expression for coupling energy, Δ is an effective energy gap for the superconductors. When the noise in the circuit becomes larger than the coupling energy, the relative phase ($\Delta\gamma$) is unrestrained and I averages to zero. Thermal noise reaching the junction from our (room-temperature) circuits is about $10^{-20}R$ (J). Comparing this noise with the coupling energy, it is clear that there is an upper limit to the junction resistance of about 10-20 Ω, beyond which no Josephson dc current will be observed.

A voltage impressed on these "normal" junctions should still produce a Josephson alternating current even though noise has suppressed the zero-voltage current. For "normal" junctions this noise will produce a considerable frequency fluctuation[4] in any ac Josephson effect. However, we will still expect to observe ac Josephson effects from these junctions whenever this frequency uncertainty can be made relatively negligible. Stabilization of this type is accomplished in these experiments by closely coupling an electromagnetic cavity to the junction. At certain frequencies the cavity resonantly enhances the voltage generated from the fluctuating Josephson current. These voltages then feed back into the junction, tending to synchronize the phases[4] and produce Fiske[5] type modes, the particular mode being determined by the external cavity rather than the junction itself.

Our experiments were done using a superconducting-strip line cavity connecting two junctions. If two small identical junctions are connected in parallel by superconducting links (forming an "interferometer"),[6] the total supercurrent flow through the pair is

$$I_T = I_0 \frac{\sin[(e/\hbar)\varphi_J]}{(e/\hbar)\varphi_J} \cos\left(\frac{1}{2\hbar}\oint p\,dx\right) \sin(\Delta\gamma_0). \qquad (2)$$

We choose to neglect the spatial variation of voltage within the (small) junctions at the relatively low frequencies involved in these experiments. However, variation in phase of the rf voltage along the superconducting links is not negligible, since the cavity formed by these links can support many electromagnetic modes. The quantum phase difference ($\Delta\gamma_0$) is related to voltage (V) across the barriers by (d/dt)

$\gamma(\Delta\gamma_0) = (2e/\hbar)V$, if the junctions are in phase (even modes). Total supercurrent flow for these even modes is

$$I_T = I_0 \frac{\sin[(e/\hbar)\varphi_J]}{(e/\hbar)\varphi_J} \cos\left(\frac{e}{\hbar}\varphi_T\right) \sin\left(\frac{2e}{\hbar}\int V dt + \alpha\right), \quad (3)$$

where φ_T is the total flux linking the device. In the "normal" state, the integration constant (α) is random and I_T averages to zero. Coupling these junctions to a cavity generates voltages from these random currents which are resonantly enhanced at certain frequencies. These voltages feed back to the junctions and, when large enough to overcome the noise fluctuation, will cause a coherent modulation. Under these conditions the direct current through a "normal" interferometer resulting from the zero-frequency sideband associated with a voltage $V = V_{dc} + v\cos\omega t$ is

$$I_T = I_0 \frac{\sin[(e/\hbar)\varphi_J]}{(e/\hbar)\varphi_J} \cos\left(\frac{e}{\hbar}\varphi_T\right) J_1\left(\frac{v}{V_{dc}}\right), \quad (4)$$

since $\omega = (2e/\hbar)V_{dc}$.

In our experiments the dc current-voltage characteristic of a "normal" interferometer was determined, in which the synchronizing rf voltage (v) was generated from the junctions themselves. Interferometers were fabricated (Fig. 1) by connecting two junctions with a folded superconducting strip line. The Josephson barriers were formed by oxidizing niobium sheet (0.998 purity) for 17 h in water saturated oxygen at about 20°C. Junctions ($\frac{1}{4}$ mm square) were completed by the overlaid tin strip line. For the data given here the strip line was 1.33 m long. This strip line is an electromagnetically resonant structure producing voltage maxima from a current source when the strip-line length (L) is an integral number of half-wavelengths long. Josephson junctions at the ends of the line are current sources at a frequency $\omega = (2e/\hbar)V_{dc}$. An applied steady voltage (V_{dc}) will thus produce an rf voltage (v) at the junctions. The magnitude of this rf voltage will depend on the Q of the strip line and the frequency, having maxima whenever the Josephson frequency matches an impedance resonance frequency of the strip line. Resonances of the rf voltage (corresponding to odd modes of electromagnetic phase) occur when-

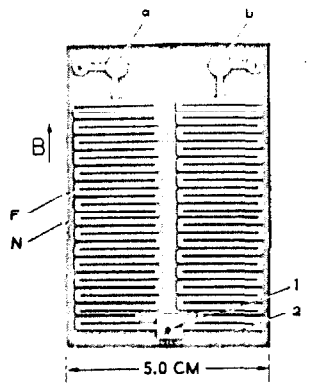

FIG. 1. Superconducting interferometer. This interferometer was fabricated by evaporating a folded tin film (~1300 Å) (F), over a Formvar-coated ($\delta = 6700 \pm 500$ Å), niobium-sheet (N) ground plane. The resulting superconducting strip line (length 1.33 m) connects Josephson junctions at (a) and (b). Voltage is measured between points (1) and (2) at which current is introduced into the device. The direction of the magnetic field is shown by arrow (B).

ever the steady voltage (V_{dc}) is

$$V_{dc} = (2N-1)\frac{h}{2e}\frac{c}{2L}\left[\frac{\delta}{\epsilon(\delta+l)}\right]^{1/2}, \quad (5)$$

when N is an integer, $\epsilon = 2.8$ is the tabulated dielectric constant of Formvar at 10^8 Hz, and δ is the strip-line spacing. The total field penetration (l) into the superconductors was determined to be 1550 ± 100 Å from measurements on the Josephson diffraction of a single junction. When the induced voltage (v) dominates the noise, the result will be a self-stimulated "step structure" in the dc current at finite voltages, similar to that first observed by Fiske[6] for single junctions. Here, however, the strip-line cavity is necessary to establish coherence (through the electromagnetic field) intrinsically lacking in the junctions because of noise.

A steady current supplied to such a "normal" interferometer will induce voltages at the junctions. The steady, "resistive" voltage will be augmented by rf voltages (generated from the junctions) which show maximum resonant enhancement at values of V_{dc} given by expression (5). These self-stimulated rf voltages will induce a structure in the current-voltage characteristic described by Eq. (4).

Such structure has been observed (Fig. 2) in a "normal" interferometer of length $L = 1.33$

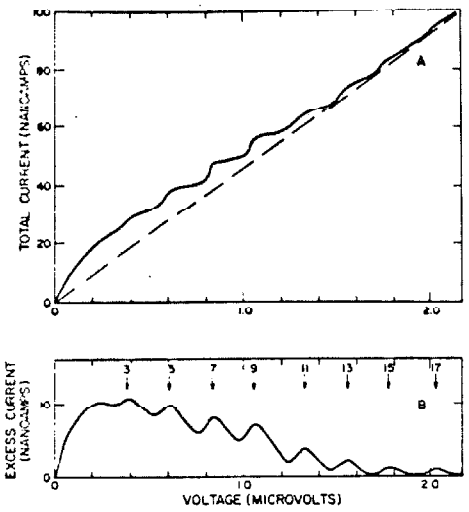

FIG. 2. (a) Current-voltage characteristic of this interferometer at 1.3°K. Magnetic flux has been chosen to maximize this mode structure. (b) Excess current-voltage characteristic: This excess current is modulated by magnetic flux in a manner expected from a Josephson current; however, these "normal" Josephson junctions show no detectable zero-voltage current.

m, where the fundamental frequency $\nu = c/2L \times [\delta/\epsilon(\delta+l)]^{1/2} = 61$ Mc/sec^{-1}. Figure 2(a) is the total direct current through the interferometer shown versus the voltage across the device. In this case, the flux has been chosen to maximize this particular current-voltage structure. Since the symmetry of the electromagnetic modes in the cavity is determined by the relative phases of the junctions, other modes (and I-V characteristics) can be tuned in by adjusting to an appropriate value of magnetic flux.

Figure 2(b) displays the excess current (above the background current) versus voltage. Evidently, to a resolution of $\frac{1}{3}$ nA, there is no zero-voltage Josephson current in this device, although an excess Josephson current of up to 10 nA appears at finite voltages. The average observed voltage spacing between modes, $\Delta V = 0.23$ μV, corresponds well to that expected from (5):

$$(h/2e)(c/L)[\delta/\epsilon(\delta+l)]^{1/2} = 0.25 \ \mu\text{V}.$$

The location of the arrows identifying the current maxima were obtained from the derivative (dV/dI vs V) curve. However, this particular labeling of modes in terms of the number of half-wavelengths in the strip line is somewhat arbitrary, since the mode spacing does not extrapolate correctly to zero voltage, probably displaying our lack of accurate knowledge of the strip-line termination.

At a given voltage the excess current is a function of magnetic flux (φ). The amplitude modulation of a single peak of Fig. 2(b) shows the expected dependence on flux. Both diffraction and interference effects have been seen, as well as the appearance of both even and odd electromagnetic modes at appropriate flux values. An independent area determination of such large interferometers is particularly imprecise; however, the observed flux period for these larger devices has been $(1.9 \pm 0.6) \times 10^{-7}$ G cm^2.

This Letter reports the observation of self-stimulated phase coherence effects in "normal" Josephson junctions and provides a consistent interpretation of the quantitative behavior. Although this effect in junctions is consistent with the microwave enhancement of critical current in superconducting bridges,[7] the direct relationship is not yet clear. These "normal" junctions have been utilized here to demonstrate quantum phase coherence in tin films at distances up to 1.33 m. A study of the interaction of the system with more complex electromagnetic modes and traveling waves is in progress.

---

[1]B. D. Josephson, Phys. Letters 1, 251 (1962).
[2]B. D. Josephson, Advan. Phys. 14, 419 (1965).
[3]P. W. Anderson and J. M. Rowell, Phys. Rev. Letters 10, 230 (1963).
[4]P. W. Anderson, in Lectures on the Many Body Problem, edited by E. R. Caianiello (Academic Press, Inc., New York, 1964), pp. 113-135.
[5]M. D. Fiske, Rev. Mod. Phys. 36, 221 (1964); D. D. Coon and M. D. Fiske, Phys. Rev. 138, A744 (1965).
[6]R. C. Jaklevic, J. Lambe, A. H. Silver, and J. E. Mercereau, Phys. Rev. Letters 12, 159 (1964).
[7]A. F. G. Wyatt, V. M. Dmitriev, W. S. Moore, and F. W. Sheard, Phys. Rev. Letters 16, 1166 (1966); A. H. Dayem, private communication.